



TOTAL IONIZING DOSE TEST REPORT

No. 03T-RT54SX7S-T25KS006

April 25, 2003

J.J. Wang
(408) 522-4576
jih-jong.wang@actel.com

I. SUMMARY TABLE

Parameter	Tolerance
1. Gross Functionality	Passed 100 krad(Si)
2. I _{cc}	Passed 66.8 krad(Si) on 25 mA spec, approximately 120 mA after 100 krad(Si) and annealing
3. Input Threshold (V _{TIL} /V _{IH})	Passed 100 krad(Si)
4. Output Drives (V _{OL} /V _{OH})	Passed 100 krad(Si)
5. Propagation Delays	Passed 72.98 krad(Si) on 10% degradation, 100 krad(Si) on 20% degradation
6. Transition Time	Passed 100 krad(Si)

II. TOTAL IONIZING DOSE (TID) TESTING

A. Device Under Test (DUT) and Irradiation

Table 1 lists the DUT information and irradiation conditions.

Table 1. DUT information and irradiation conditions

Part Number	RT54SX72S
Package	CQFP256
Foundry	Matsushita Electronics Corporation
Technology	0.25 μ m CMOS
DUT Design	TDSX72CQFP256_2Strings
Die Lot Number	T25KS006
Quantity Tested	5
Serial Number	13716, 13754, 13772, 13776, 13789
Radiation Facility	Defense Microelectronics Activity
Radiation Source	Co-60
Dose Rate	1 krad(Si)/min ($\pm 5\%$)
Irradiation Temperature	Room
Irradiation and Measurement Bias (V _{CC1} /V _{CCA})	Static at 5.0 V/2.5 V

B. Test Method

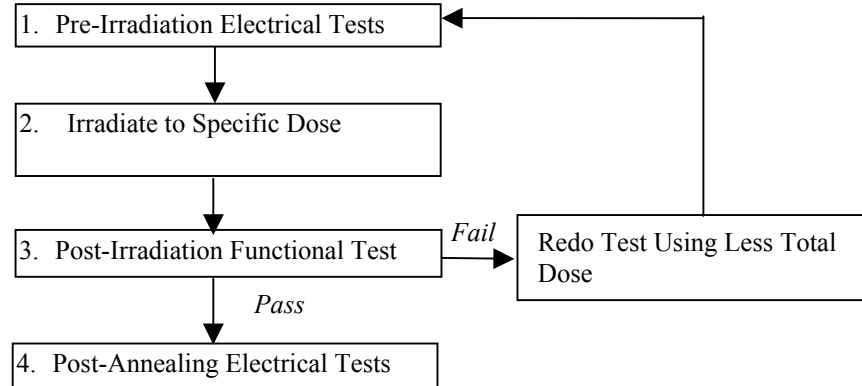


Fig 1 Parametric test flow chart

The parametric tests follow the military standard test method 1019.5. Fig 1 shows the testing flow. The time dependent effect (TDE) of this product was previously evaluated by comparing the results of a high dose rate (1 krad(Si)/min) against the results of a low dose rate (1 krad(Si)/hr). No adverse TDE was observed. Therefore the accelerated aging test (rebound test) is omitted in this test. Room temperature annealing were performed after irradiation to total dose of 100 krad(Si). Every DUT was biased and at static biased during annealing except DUT 13176 that was dynamically running for one day during the 2-week annealing period. As shown in the results in the following sections, I_{CC} and propagation degradation of DUT 13176 are much improved by annealing comparing to the other DUT. The reason is that the dynamical running raised the temperature and enhanced the annealing effect.

C. Electrical Parameter Measurements

A high utilization design (TDSX72CQ256_2Strings) to address total dose effects in typical space applications is used. The circuit schematics are shown in appendix A.

Table 2 lists the electrical parameters measured. The functionality is measured pre-irradiation, post-irradiation, and post-annealing on the output pin (O_AND3 or O_AND4) of the two combinatorial buffer-strings and on the output pins (O_OR4 and O_NAND4) of the shift register. The in-flux I_{CC} is measured on the power supply of the logic-array (I_{CCA}) and I/O (I_{CCI}) respectively.

The input logic thresholds (V_{TIL}/V_{IH}) and output drives (V_{OL}/V_{OH}) are measured pre-irradiation and post-annealing on a combinational net, the input pin DA to the output pin QA0. The propagation delays are measured pre-irradiation and post-annealing on the buffer strings in three stages with 50, 500 and 560 buffers respectively. The delay is defined as from the input CLOCK to the output. The transient time is measured pre-irradiation and post-annealing on O_AND4. The buffer string is controlled by clocking flip-flops during the propagation delay and transient measurements.

Unused inputs are grounded with an 1 M ohm resistor during irradiation and an 1.2K ohm resistor during annealing.

Table 2. Logic design for parametric tests

Parameter/Characteristics	Logic Design
1. Functionality	All key architectural functions (pins O_AND3, O_AND4, O_OR3, O_OR4, and O_NAND4)
2. I_{CC} (I_{CCA}/I_{CCI})	DUT power supply
3. Input Threshold (V_{TIL}/V_{IH})	TTL compatible input buffer (pin DA to QA0)
4. Output Drive (V_{OL}/V_{OH})	TTL compatible output buffer (pin DA to QA0)
5. Propagation Delay	String of buffers (pin LOADIN to Y50, Y500, or O_AND4)
6. Transition Time	D flip-flop output (O_AND4)

III. TEST RESULTS

A. *Functionality*

Every DUT passed the gross functional test at pre-irradiation, post-irradiation, and post-annealing.

B. I_{CC}

Figs 2-6 show the in-flux I_{CC} plots. For the same accumulative total dose, I_{CC} at the present dose rate of 1 krad(Si)/min is significant higher than the previous results tested at lower dose rate of 1 krad(Si)/hr (see for example report No. 02T-RT54SX72S-T25KS005). At 100 krad(Si) total dose, I_{CC} (I_{CCA} and I_{CCI}) for high dose rate is averaging approximately 200 mA, while I_{CC} average for low dose rate is less than half of that.

Except DUT 13716, the average I_{CC} dropped to approximately 120 mA after annealing. I_{CC} of DUT 13716 dropped to about 60 mA, much lower than that of the other DUT because of annealing dynamically. The radiation tolerance based on the 25 mA spec has to be extracted from the annealing characteristic. Fig 7 shows the annealing characteristic of DUT 13772. The current is normalized with the peak current at 100 krad(Si) total dose. The log-log plot shows a straight line after the short initial stage. Extending the curve to 10 years mission time, the annealing factor is obtained approximately as 0.32 for I_{CCA} and 0.29 for I_{CCI} . These annealing factors are approximately the same values as those in RT54SX32S, see Fig 6 in report 03T-RT54SX32S-T25JS004. Assume that annealing factors are dependent on the product and bias voltage but relatively independent of the total dose in the range of interest, the critical total dose ($\gamma_{critical}$) for the 10-year mission to induce I_{CC} to 25 mA can be obtained by the equation,

$$I_{CCA}(\gamma_{critical}) \times 0.32 + I_{CCI}(\gamma_{critical}) \times 0.29 = 25mA$$

Where $I_{CCA}(\gamma)$ and $I_{CCI}(\gamma)$ are read from the raw data which generates Fig 4. The tolerance ($\gamma_{critical}$) is thus obtained as approximately 66.8 krad(Si). This number is believed to be overly pessimistic. Theoretically and empirically, the DUT irradiated at high dose rate and then annealed for a period to match the total mission time have significantly higher I_{CC} than that in a DUT irradiated at a low, uniform dose rate throughout the total mission time.

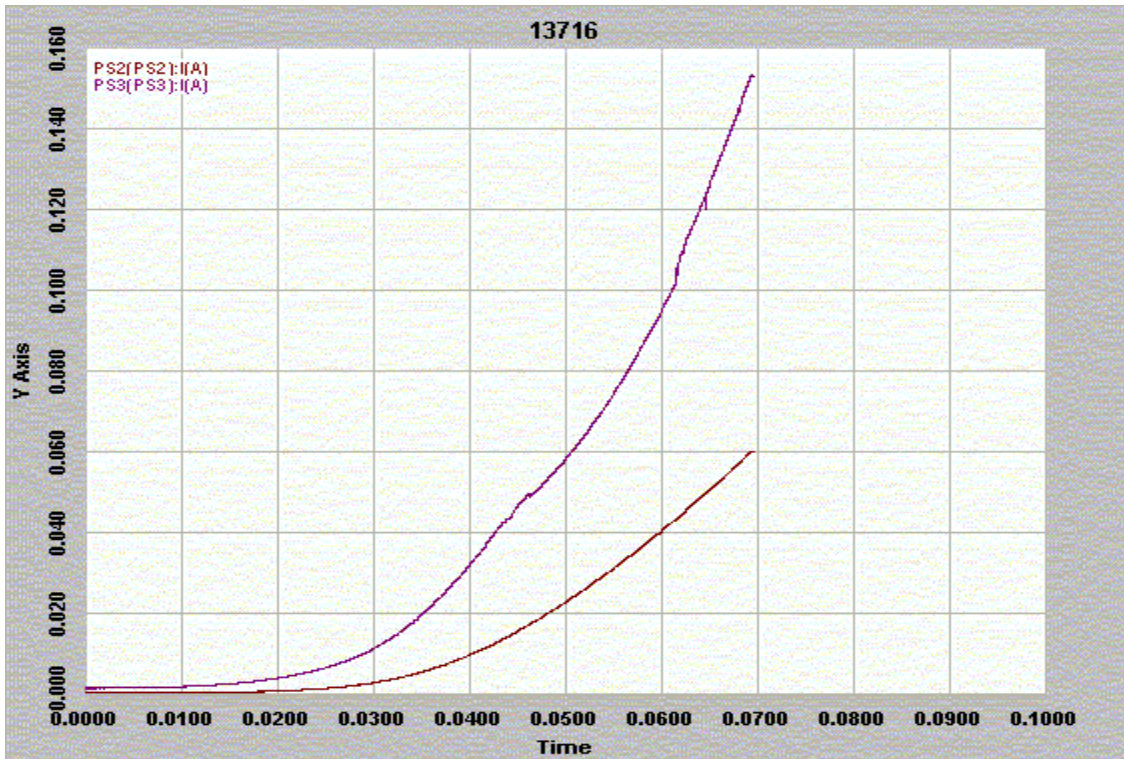


Fig 2 In-flux I_{CC} of DUT 13716, PS2 supplies I_{CCI} and PS3 supplies I_{CCA} . The current unit is amps and the time unit is days, 0.01 day is equivalent to 14.4 krad(Si). I_{CC} reaches the peak at 100 krad(Si), irradiation stops after 100 krad(Si) and I_{CC} drops due to annealing effect.

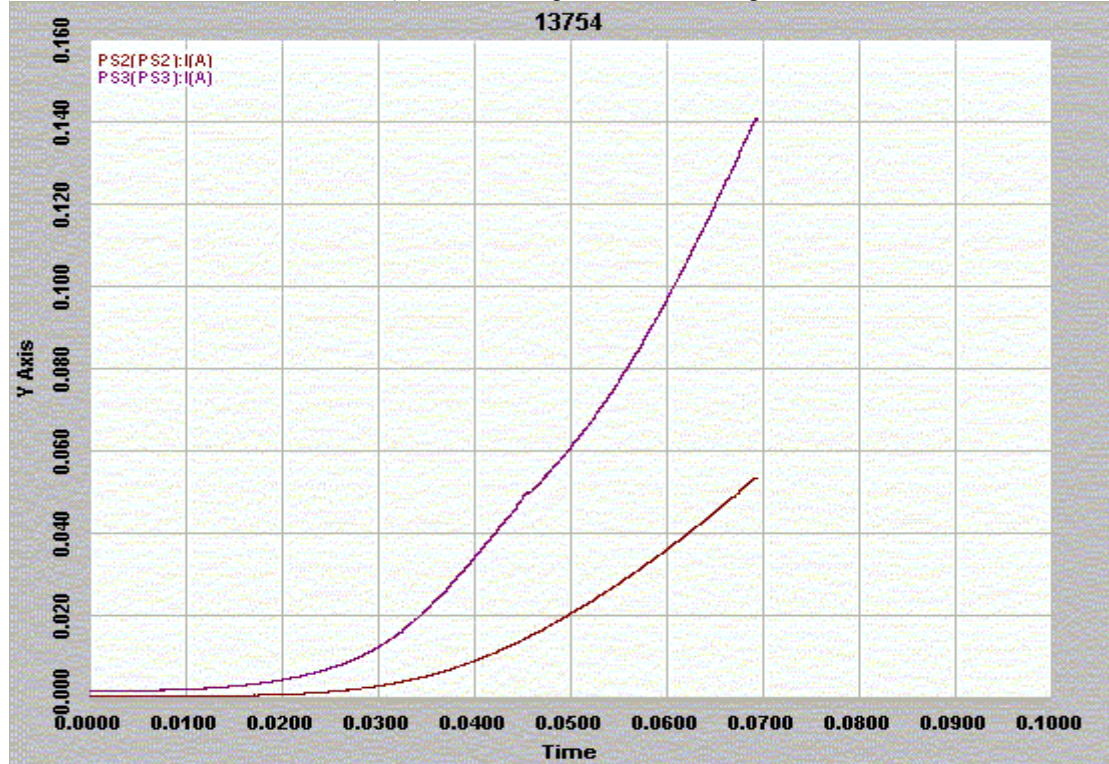


Fig 3 In-flux I_{CC} of DUT 13754, PS2 supplies I_{CCI} and PS3 supplies I_{CCA} . The current unit is amps and the time unit is days, 0.01 day is equivalent to 14.4 krad(Si). I_{CC} reaches the peak at 100 krad(Si), irradiation stops after 100 krad(Si) and I_{CC} drops due to annealing effect.



Fig 4 In-flux I_{CC} of DUT 13772, PS2 supplies I_{CCI} and PS3 supplies I_{CCA} . The current unit is amps and the time unit is days, 0.01 day is equivalent to 14.4 krad(Si). I_{CC} reaches the peak at 100 krad(Si), irradiation stops after 100 krad(Si) and I_{CC} drops due to annealing effect.



Fig 5 In-flux I_{CC} of DUT 13776, PS2 supplies I_{CCI} and PS3 supplies I_{CCA} . The current unit is amps and the time unit is days, 0.01 day is equivalent to 14.4 krad(Si). I_{CC} reaches the peak at 100 krad(Si), irradiation stops after 100 krad(Si) and I_{CC} drops due to annealing effect.



Fig 6 In-flux I_{CC} of DUT 13789, PS2 supplies I_{CCI} and PS3 supplies I_{CCA} . The current unit is amps and the time unit is minutes, 1 minute is equivalent to 1 krad(Si). I_{CC} reaches the peak at 100 krad(Si), irradiation stops after 100 krad(Si) and I_{CC} drops due to annealing effect.

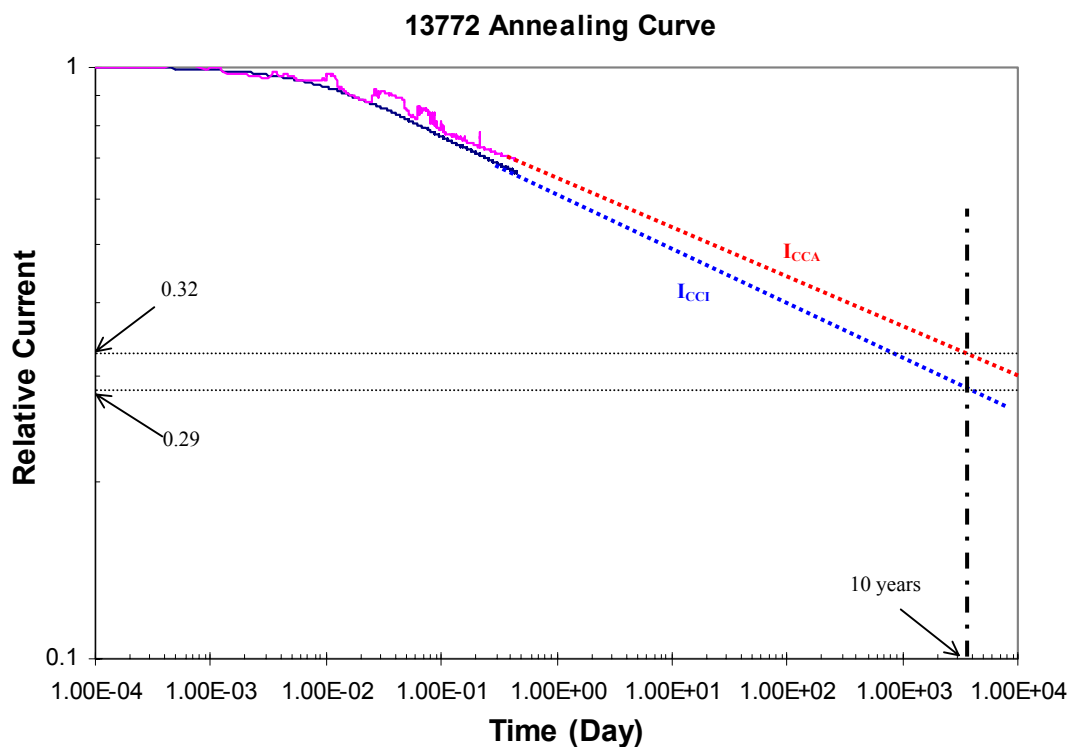


Fig 7 I_{CC} annealing curve, the dotted lines are extrapolations for the 10 years flight mission.

C. Input Logic Threshold (V_{IL}/V_{IH})

Table 4 lists the pre-irradiation and post-annealing input logic threshold for each DUT. All measured data are well within the spec limits.

Table 4 Pre-irradiation and post-annealing input logic threshold in volts

DUT	Pre-Irradiation		Post-Annealing	
	V_{IL}	V_{IH}	V_{IL}	V_{IH}
13716	1.364	1.557	1.31	1.57
13754	1.366	1.515	1.38	1.65
13772	1.341	1.489	1.29	1.56
13776	1.363	1.523	1.32	1.57
13789	1.357	1.506	1.33	1.58

D. Output Characteristics (V_{OL}/V_{OH})

The pre-irradiation and post-annealing V_{OL}/V_{OH} are listed in table 5 and 6. The post-annealing data are well within the spec limits, and 100 krad(Si) radiation has little effect on these parameters.

Table 5 Pre-irradiation and post-annealing V_{OL} (in volts) at various sinking current

DUT	1 mA		12 mA		20 mA		50 mA		100 mA	
	Pre-rad	Pos-an								
13716	0.009	0.009	0.104	0.110	0.173	0.180	0.437	0.440	0.900	0.910
13754	0.009	0.009	0.105	0.105	0.175	0.175	0.442	0.443	0.910	0.912
13772	0.009	0.009	0.103	0.104	0.172	0.174	0.435	0.438	0.894	0.900
13776	0.009	0.009	0.103	0.103	0.172	0.172	0.430	0.434	0.896	0.895
13789	0.009	0.009	0.103	0.103	0.171	0.172	0.433	0.434	0.892	0.893

Table 6 Pre-irradiation and post-annealing V_{OH} (in volts) at various sourcing current

DUT	1 mA		8 mA		20 mA		50 mA		100 mA	
	Pre-rad	Pos-an								
13716	4.98	4.98	4.86	4.86	4.66	4.65	4.11	4.10	3.02	2.97
13754	4.98	4.96	4.86	4.84	4.66	4.63	4.11	4.07	3.03	2.96
13772	4.98	4.97	4.86	4.85	4.66	4.65	4.13	4.10	3.06	3.00
13776	4.98	4.98	4.86	4.86	4.66	4.65	4.12	4.10	3.04	3.00
13789	4.98	4.98	4.86	4.86	4.66	4.66	4.12	4.11	3.04	3.00

E. Propagation Delays

Tables 7 and 8 list the pre-irradiation and post-annealing propagation delays and radiation-induced degradations. The dynamically annealed DUT 13716 shows much less degradation. The worst-case degradation is within 20%. To extract the tolerance of 10% degradation, a piece-wise linear fitting curve of propagation delay against total dose is used. This approach is based on experimental data measured on SXS products. To be conservative, the worst delay of 1400 buffers stage, 18.19% is used. Although the 50 and 500 stages have slightly higher degradations, the data for 1400 buffers stage is used because it is more accurate. The piece-wise linear fitting curve has two regions, region 1 from 0 krad(Si) to 40 krad(Si) has 0% degradation, and region 2 from 40 krad(Si) to 100 krad(Si) has a slope defined in the equation,

$$\text{Slope} = \frac{\text{TPD}(\text{Max Dose}) - \text{TPD}(\text{Initial})}{\text{Maximum Dose} - 40\text{krad}}$$

Where TPD is measured in percentage. In this case, TPD(Max Dose) is 18.19%, and TPD(Initial) is 0%. The maximum dose is 100 krad(Si). The total dose corresponding to 10% degradation on the linear curve in region 2 is the standard 10% degradation tolerance, which is approximately 72.98 krad(Si).

Table 7 Low to high delays (in nanoseconds)

DUT	50 buffers stage			500 buffers stage			1400 buffers stage		
	Pre-Irra	Post-Ann	Degrad	Pre-Irra	Post-Ann	Degrad	Pre-Irra	Post-Ann	Degrad
^a 13716	62.70	66.177	5.55%	457.03	477.96	4.58%	1259.4	1328.2	5.46%
13754	62.90	68.720	9.25%	459.10	499.81	8.87%	1266.7	1418.6	11.99%
13772	62.78	68.203	8.64%	457.18	493.91	8.03%	1263.6	1385.4	9.64%
13776	62.80	69.749	11.07%	455.30	502.91	10.46%	1257.7	1411.8	12.25%
13789	62.35	71.095	14.03%	453.18	516.75	14.03%	1247.6	1447.1	15.99%

^a13716 is annealed dynamically

Table 8 High to low delays (in nanoseconds)

DUT	50 buffers stage			500 buffers stage			1400 buffers stage		
	Pre-Irra	Post-Ann	Degrad	Pre-Irra	Post-Ann	Degrad	Pre-Irra	Post-Ann	Degrad
^a 13716	56.47	60.667	7.43%	398.80	421.66	5.73%	1100.2	1154.19	4.91%
13754	55.98	64.252	14.78%	395.76	450.01	13.71%	1092.3	1243.58	13.85%
13772	54.97	62.897	14.42%	388.04	440.99	13.65%	1071.5	1207.80	12.72%
13776	56.69	65.315	15.21%	398.50	456.33	14.51%	1102.5	1259.70	14.26%
13789	55.88	66.398	18.82%	394.70	468.32	18.65%	1087.9	1285.83	18.19%

^a13716 is annealed dynamically

F. Transition Time

The pre-irradiation and post-annealing rising and falling edges are plotted in Figs 8-17. In each case, the radiation-induced degradation is almost invisible, and the transition time both before and after irradiation is always within 3 nanoseconds.

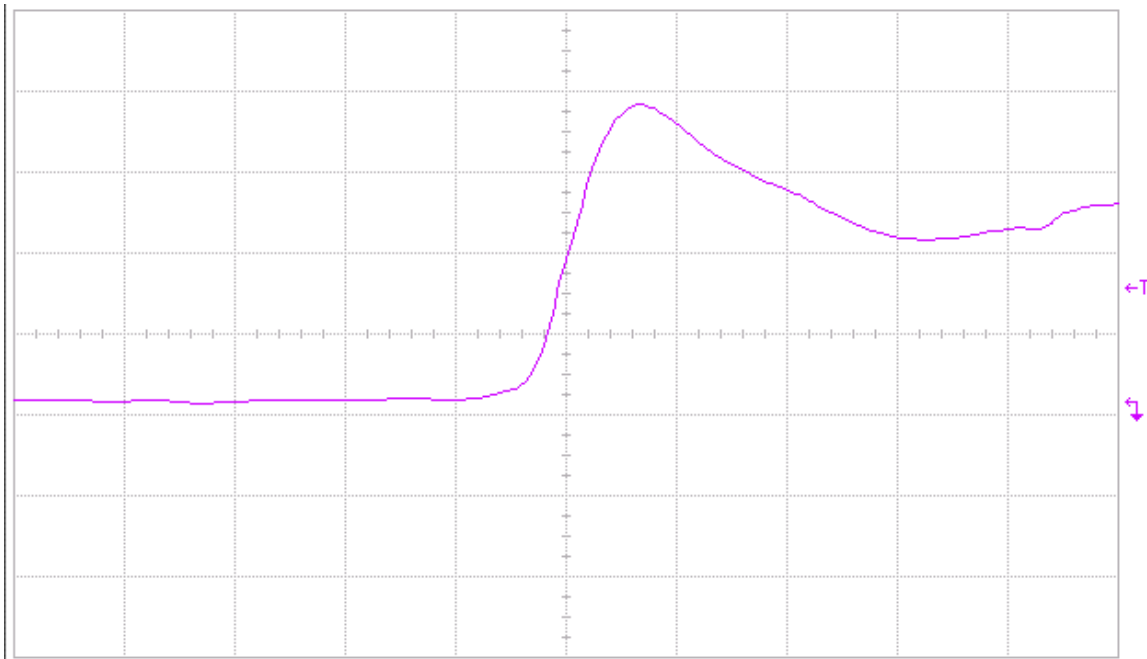


Fig 8(a) Pre-irradiation rising edge of DUT 13716, abscissa scale is 2 V/div and ordinate scale is 2 ns/div.

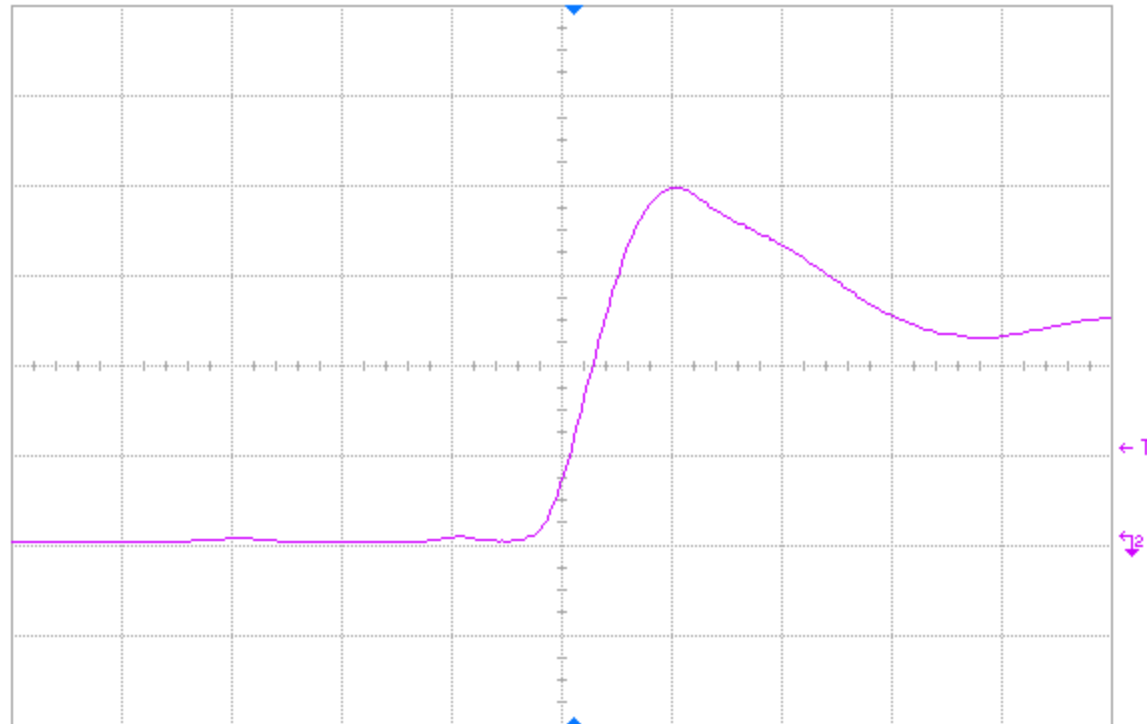


Fig 8(b) Post-annealing rising edge of DUT 13716, abscissa scale is 2 V/div and ordinate scale is 2 ns/div.

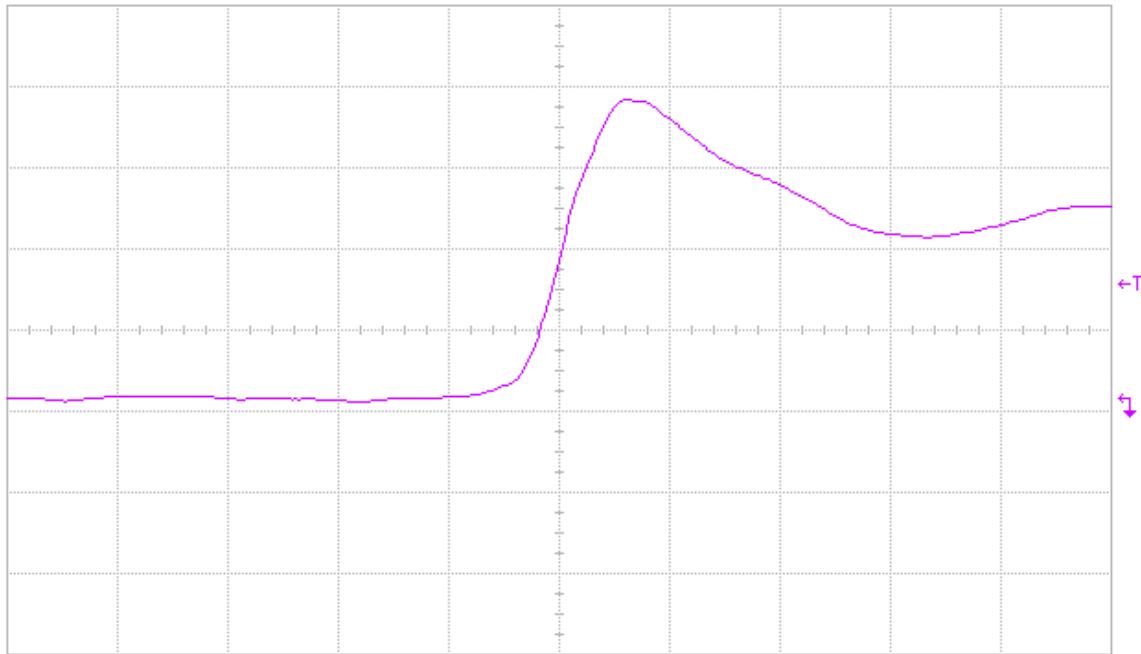


Fig 9(a) Pre-irradiation rising edge of DUT 13754, abscissa scale is 2 V/div and ordinate scale is 2 ns/div.

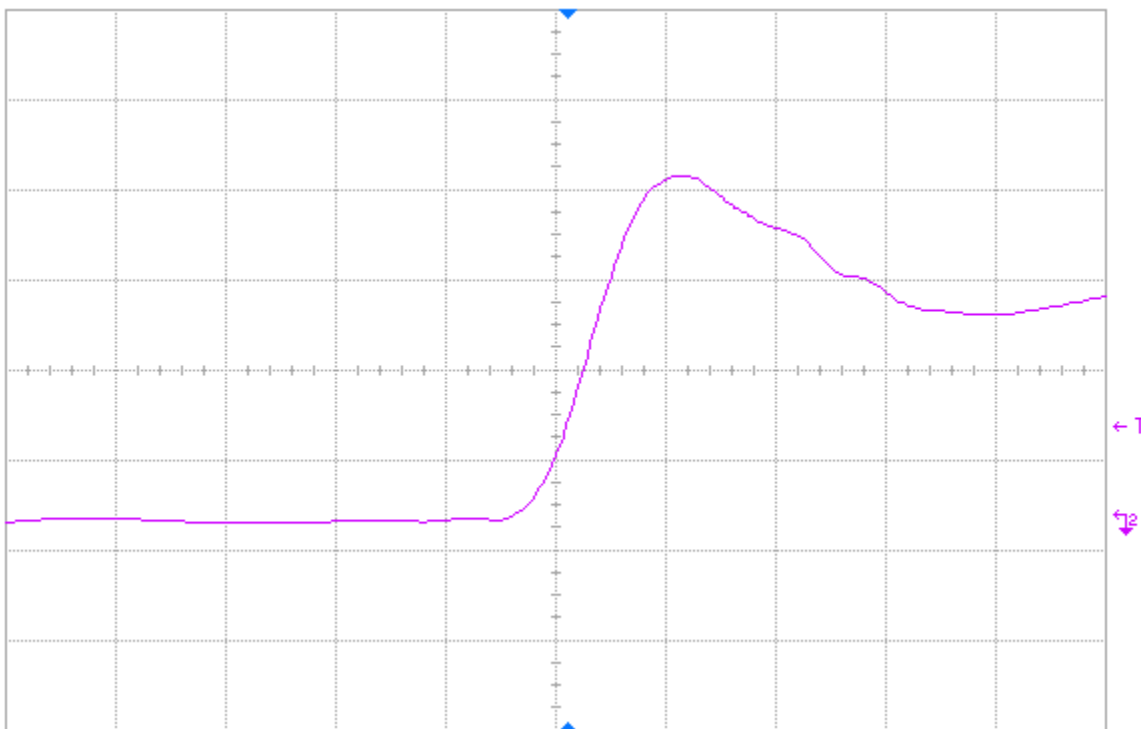


Fig 9(b) Post-annealing rising edge of DUT 13754, abscissa scale is 2 V/div and ordinate scale is 2 ns/div.

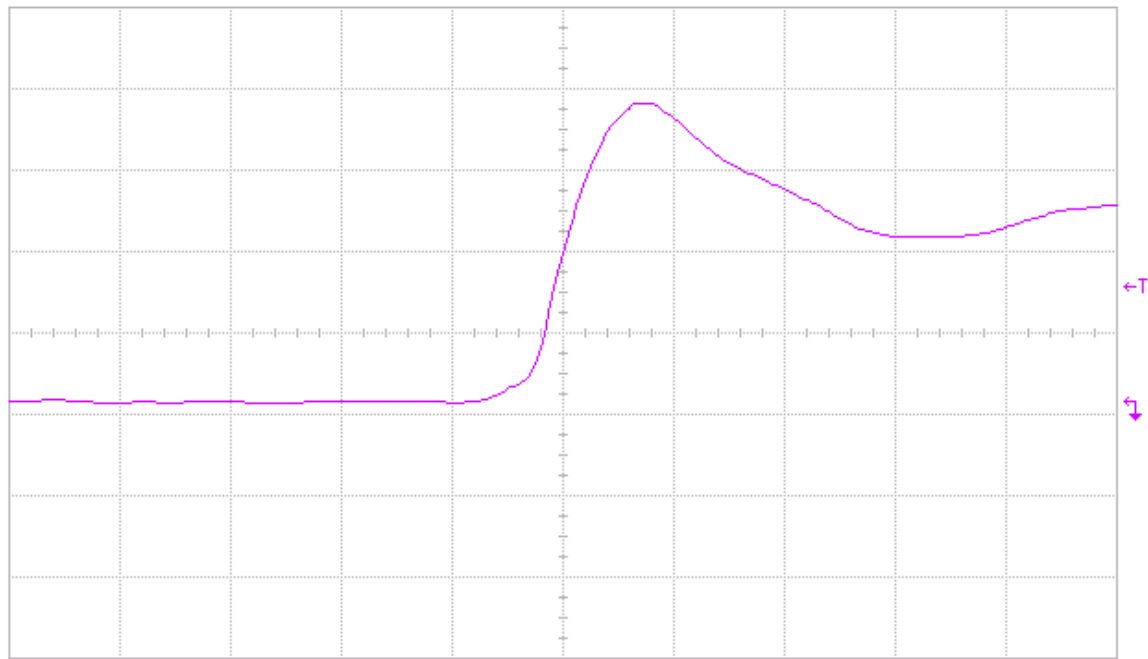


Fig 10(a) Pre-irradiation rising edge of DUT 13772, abscissa scale is 2 V/div and ordinate scale is 2 ns/div.

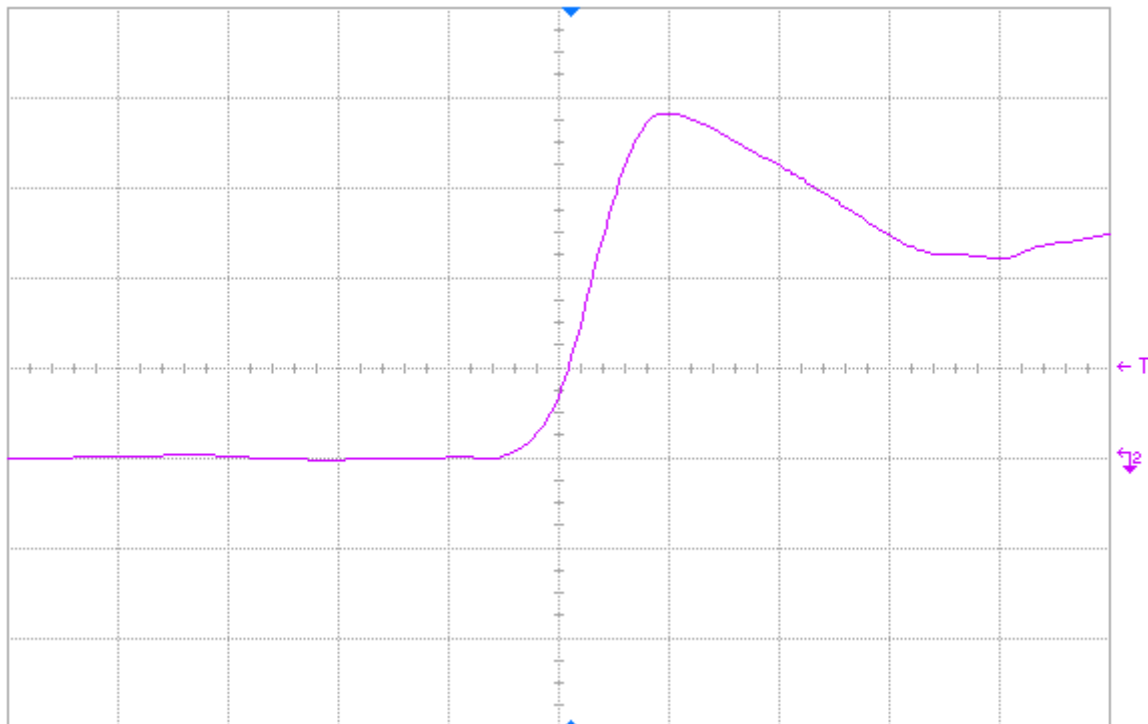


Fig 10(b) Post-annealing rising edge of DUT 13772, abscissa scale is 2 V/div and ordinate scale is 2 ns/div.

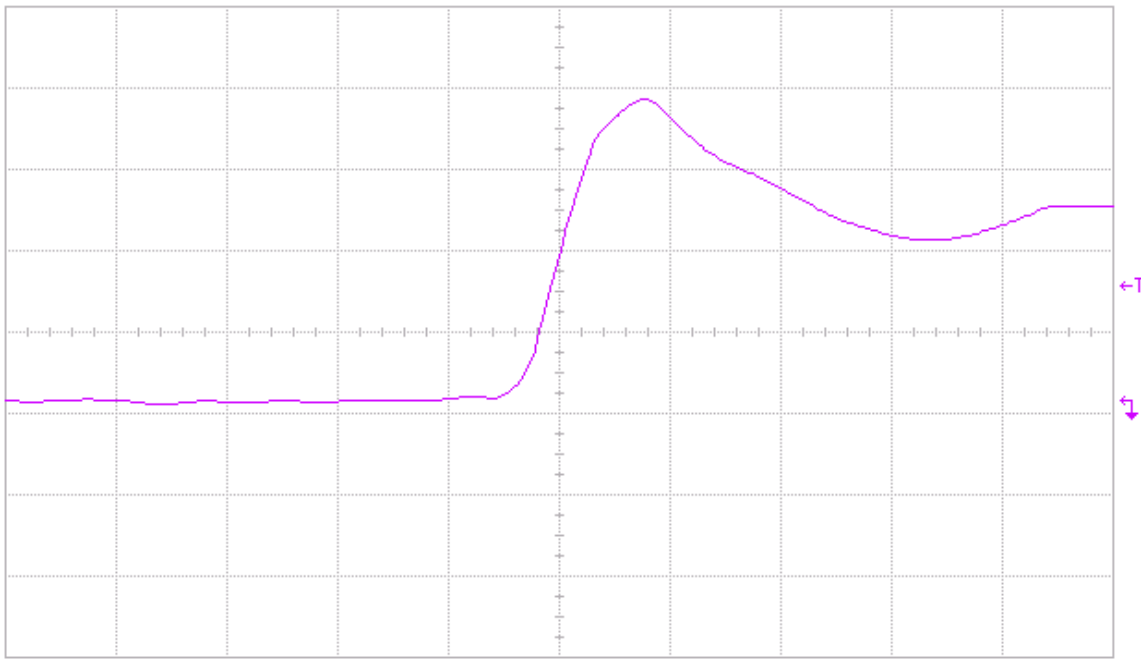


Fig 11(a) Pre-irradiation rising edge of DUT 13776, abscissa scale is 2 V/div and ordinate scale is 2 ns/div.

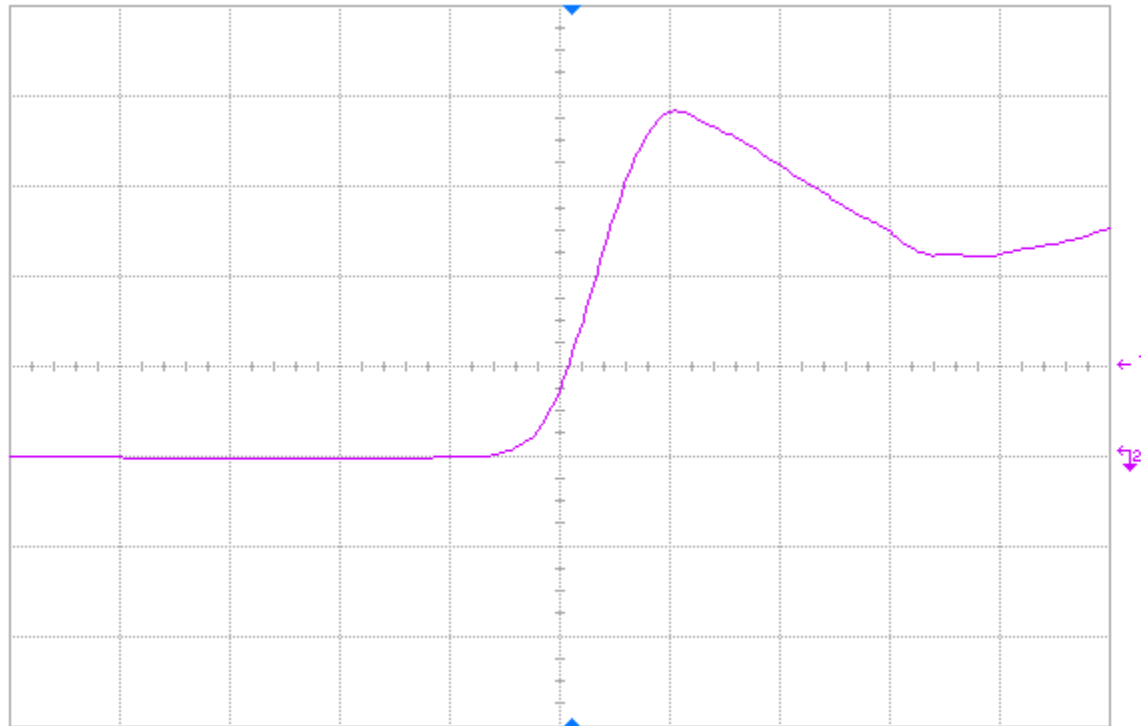


Fig 11(b) Post-annealing rising edge of DUT 13776, abscissa scale is 2 V/div and ordinate scale is 2 ns/div.

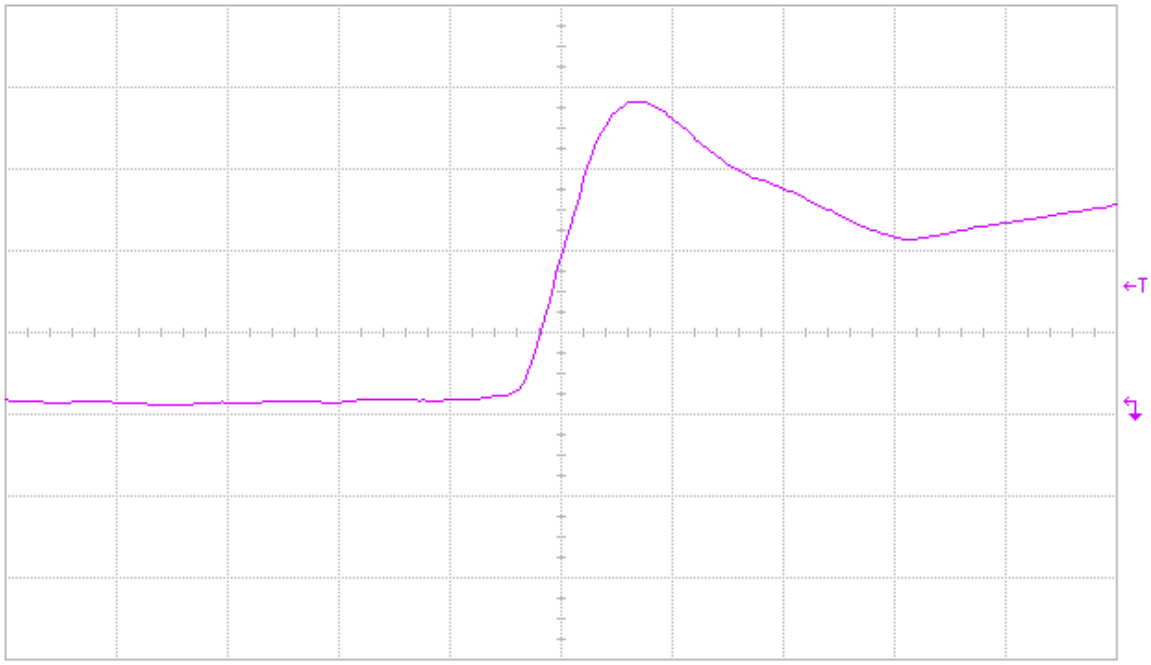


Fig 12(a) Pre-irradiation rising edge of DUT 13786, abscissa scale is 2 V/div and ordinate scale is 2 ns/div.

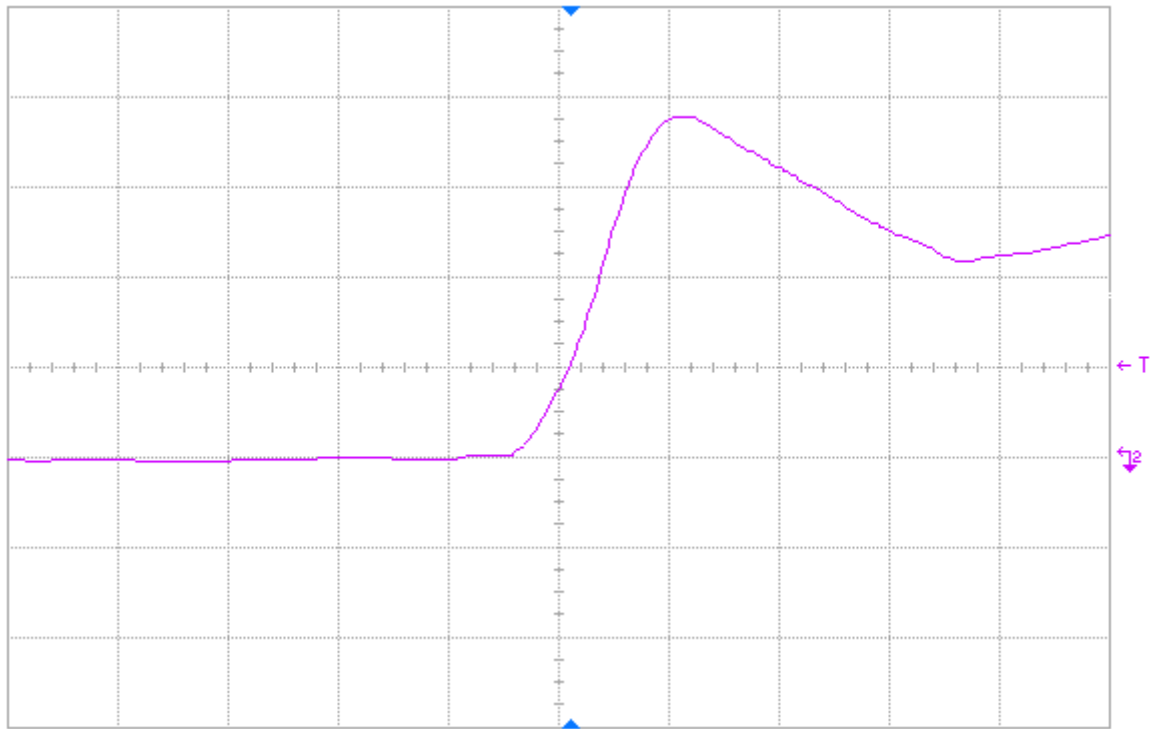


Fig 12(b) Post-annealing rising edge of DUT 13789, abscissa scale is 2 V/div and ordinate scale is 2 ns/div.

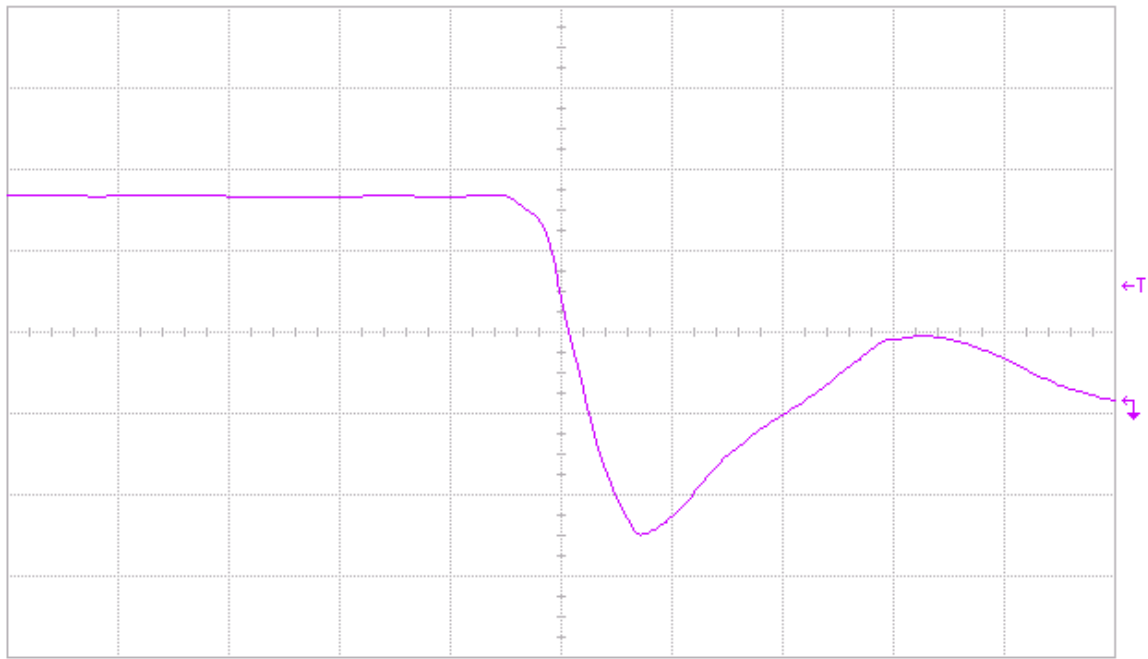


Fig 13(a) Pre-irradiation falling edge of DUT 13716, abscissa scale is 2 V/div and ordinate scale is 2 ns/div.

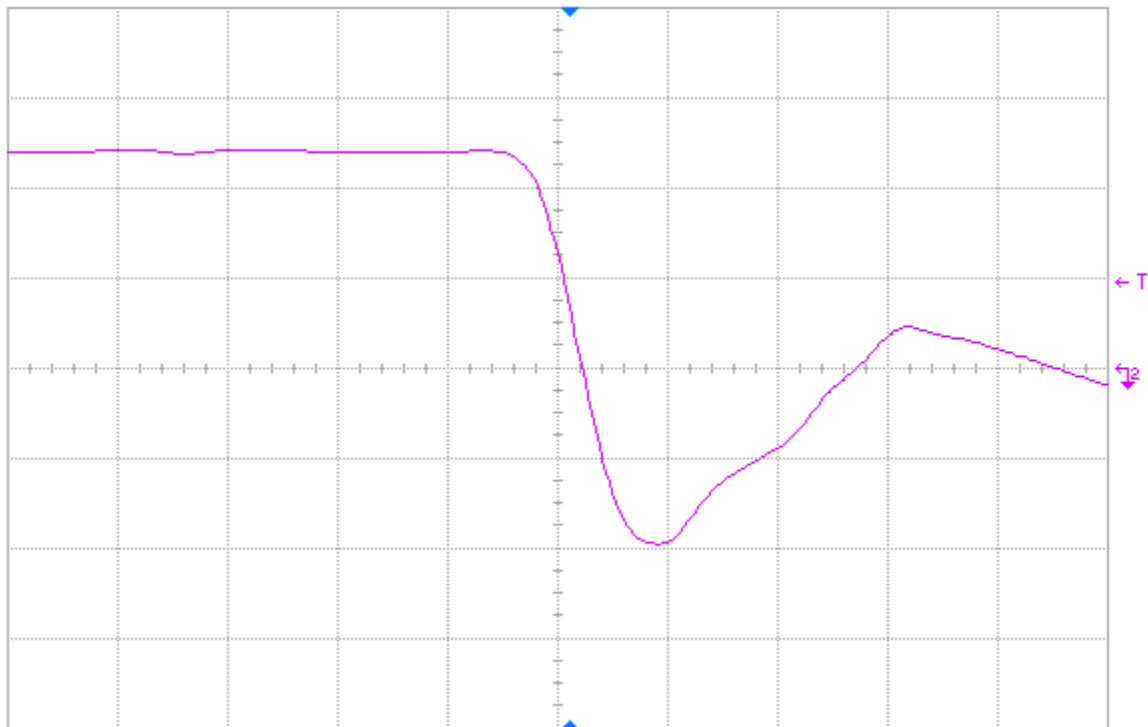


Fig 13(b) Post-annealing falling edge of DUT 13716, abscissa scale is 2 V/div and ordinate scale is 2 ns/div.

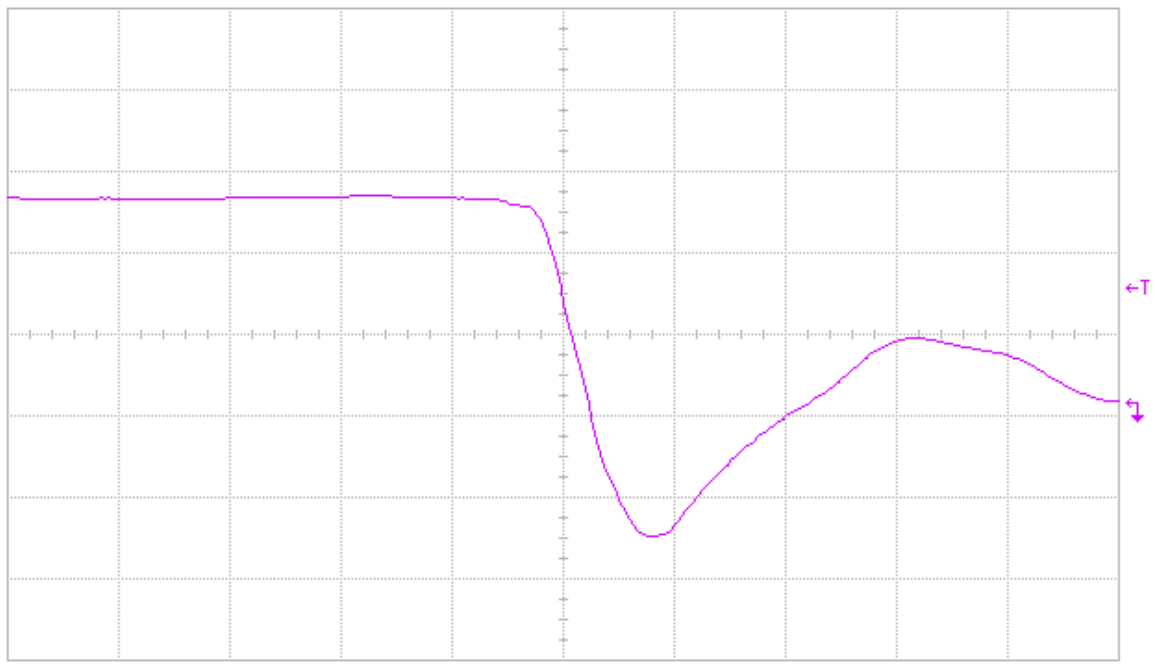


Fig 14(a) Pre-irradiation falling edge of DUT 13754, abscissa scale is 2 V/div and ordinate scale is 2 ns/div.

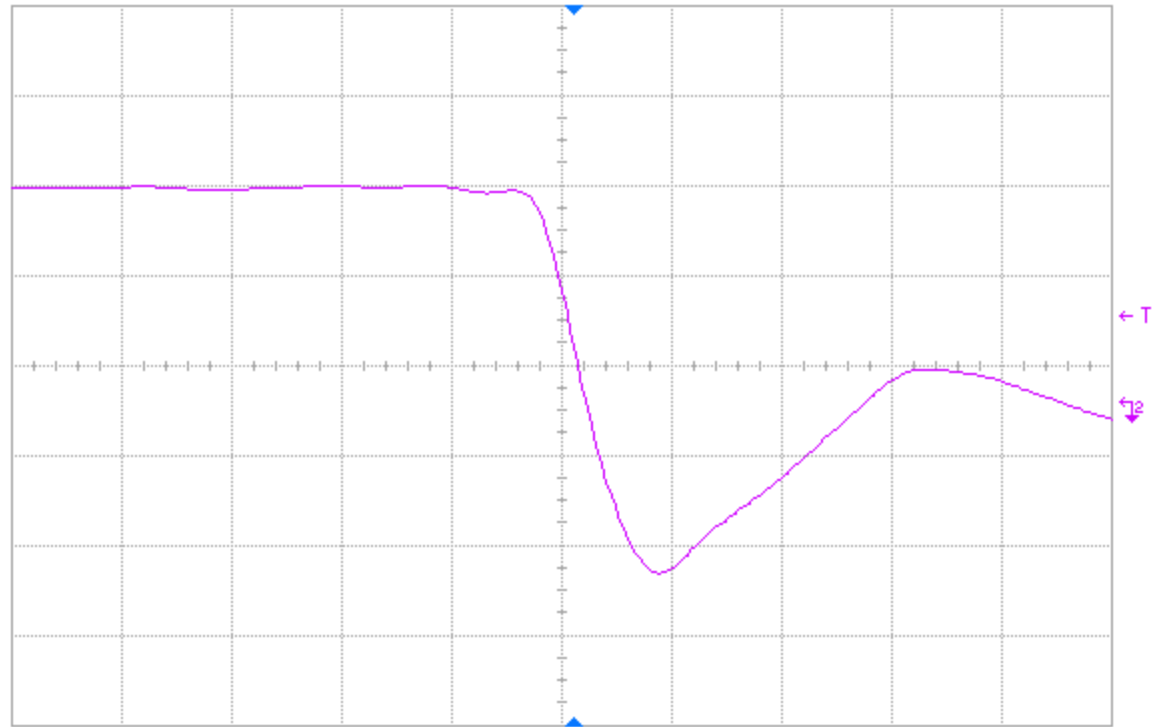


Fig 14(b) Post-annealing falling edge of DUT 13754, abscissa scale is 2 V/div and ordinate scale is 2 ns/div.

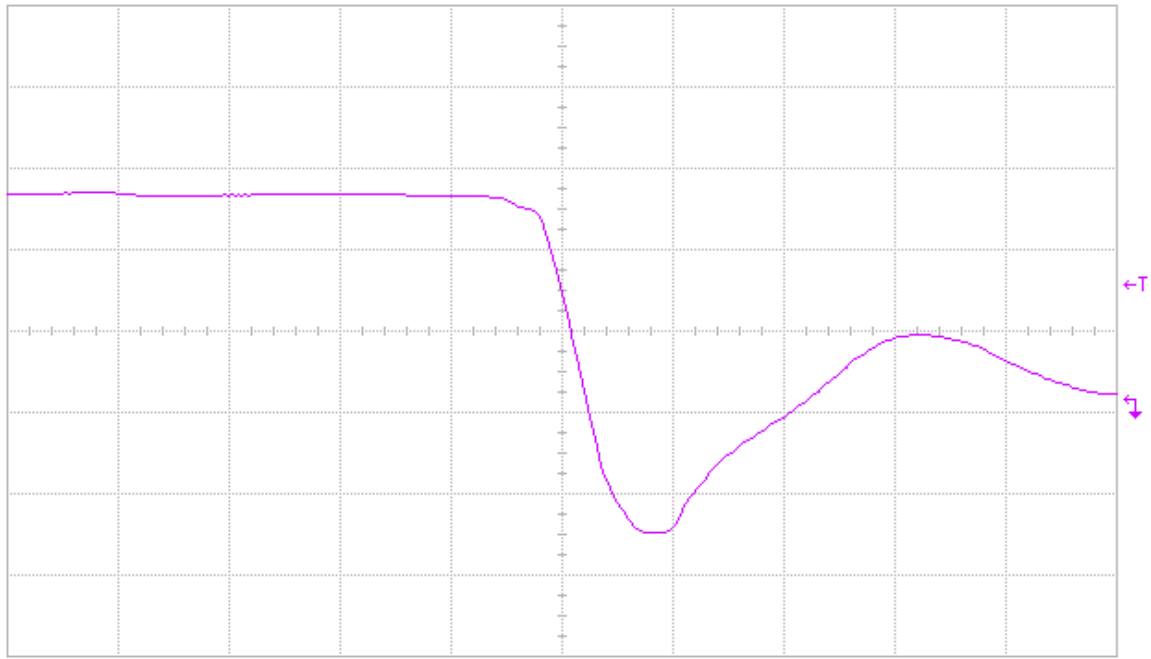


Fig 15(a) Pre-irradiation falling edge of DUT 13772, abscissa scale is 2 V/div and ordinate scale is 2 ns/div.

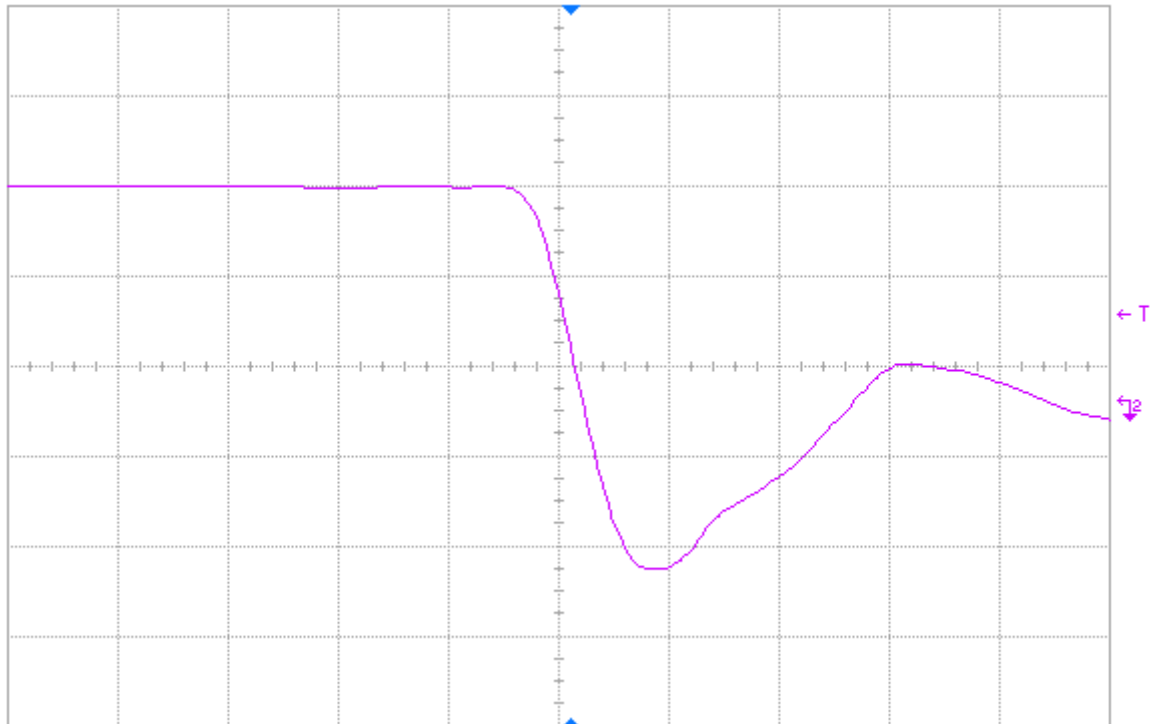


Fig 15(b) Post-annealing falling edge of DUT 13772, abscissa scale is 2 V/div and ordinate scale is 2 ns/div.

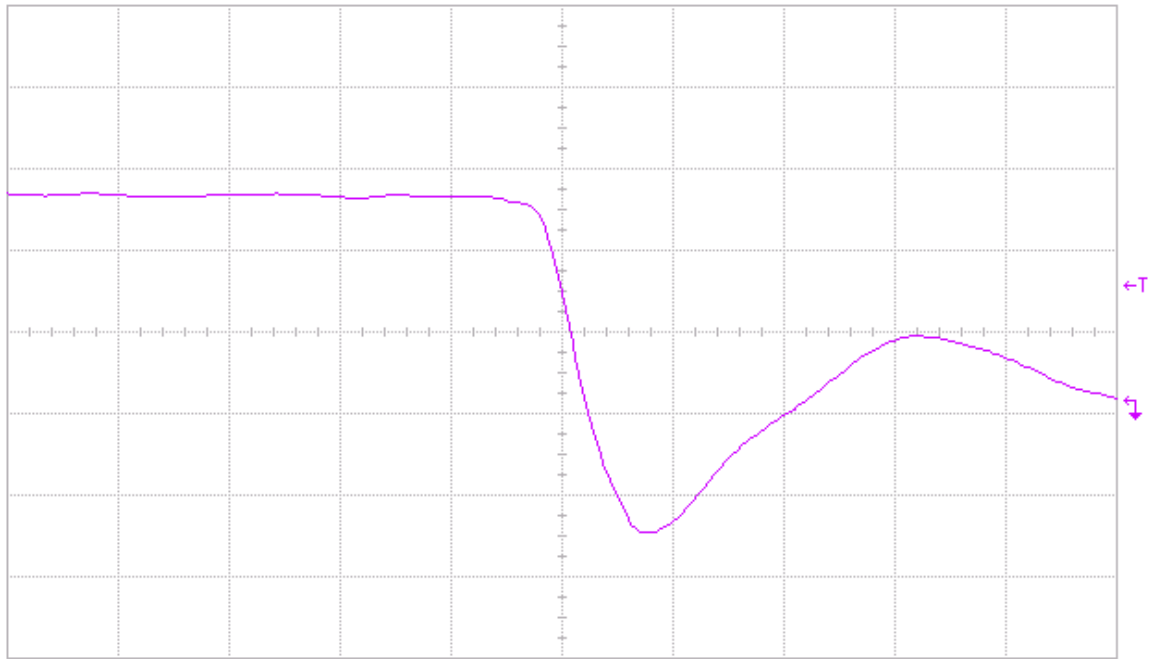


Fig 16(a) Pre-irradiation falling edge of DUT 13776, abscissa scale is 2 V/div and ordinate scale is 2 ns/div.

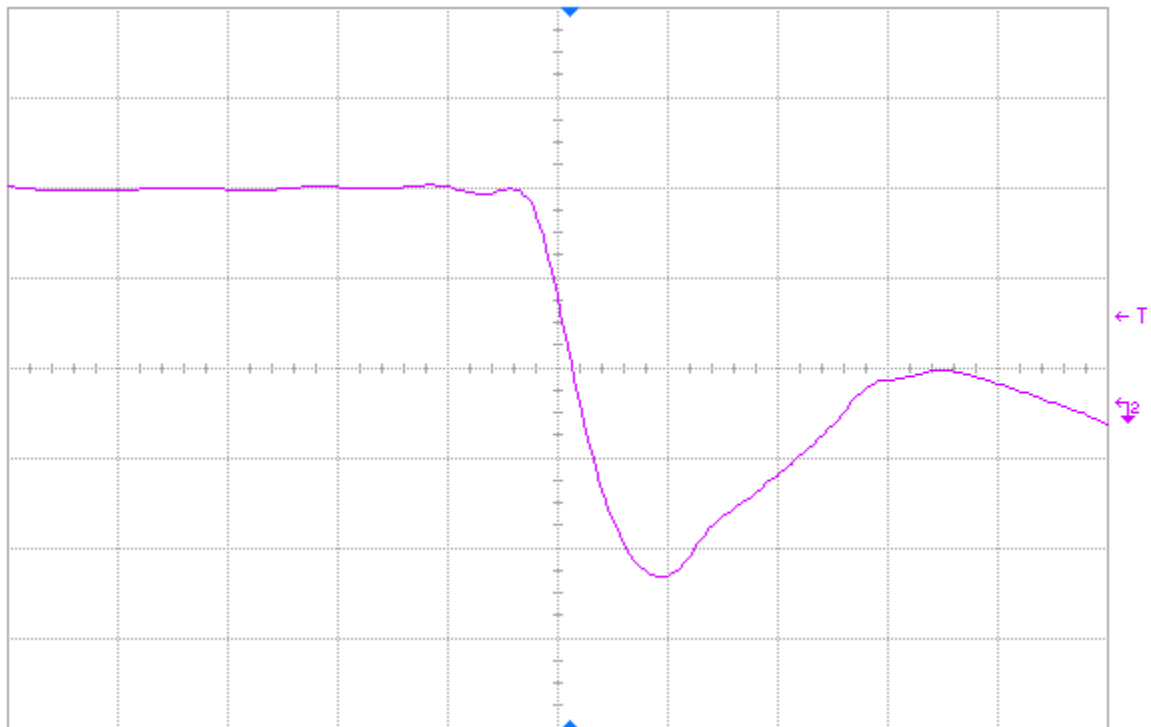


Fig 16(b) Post-annealing falling edge of DUT 13776, abscissa scale is 2 V/div and ordinate scale is 2 ns/div.

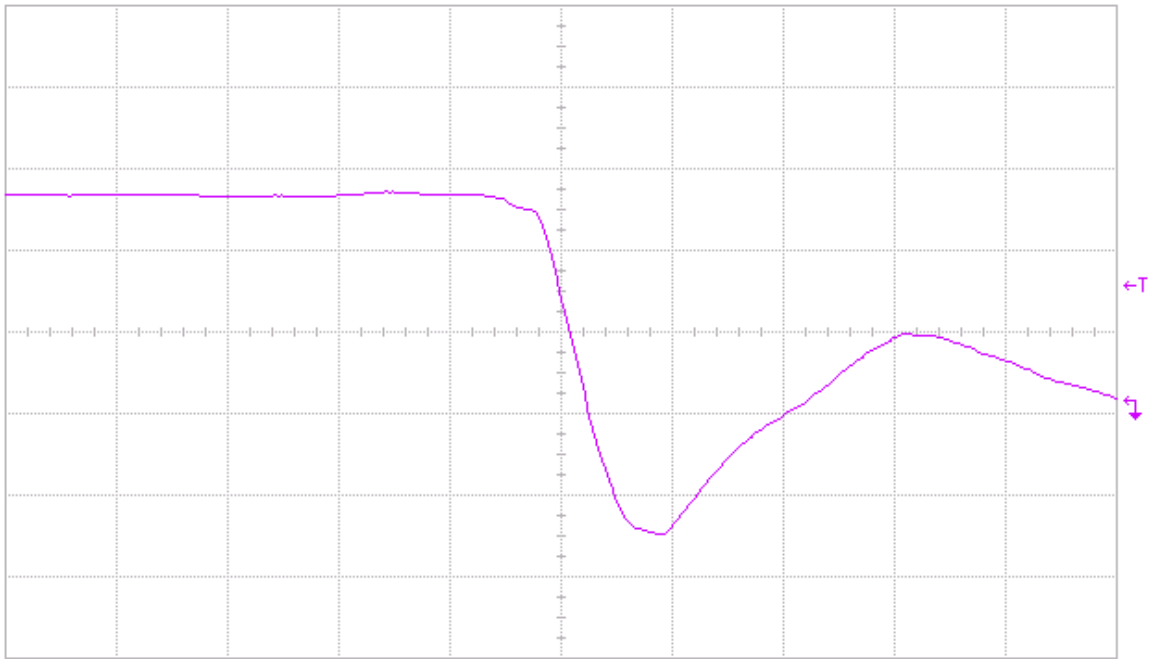


Fig 17(a) Pre-irradiation falling edge of DUT 13789, abscissa scale is 2 V/div and ordinate scale is 2 ns/div.

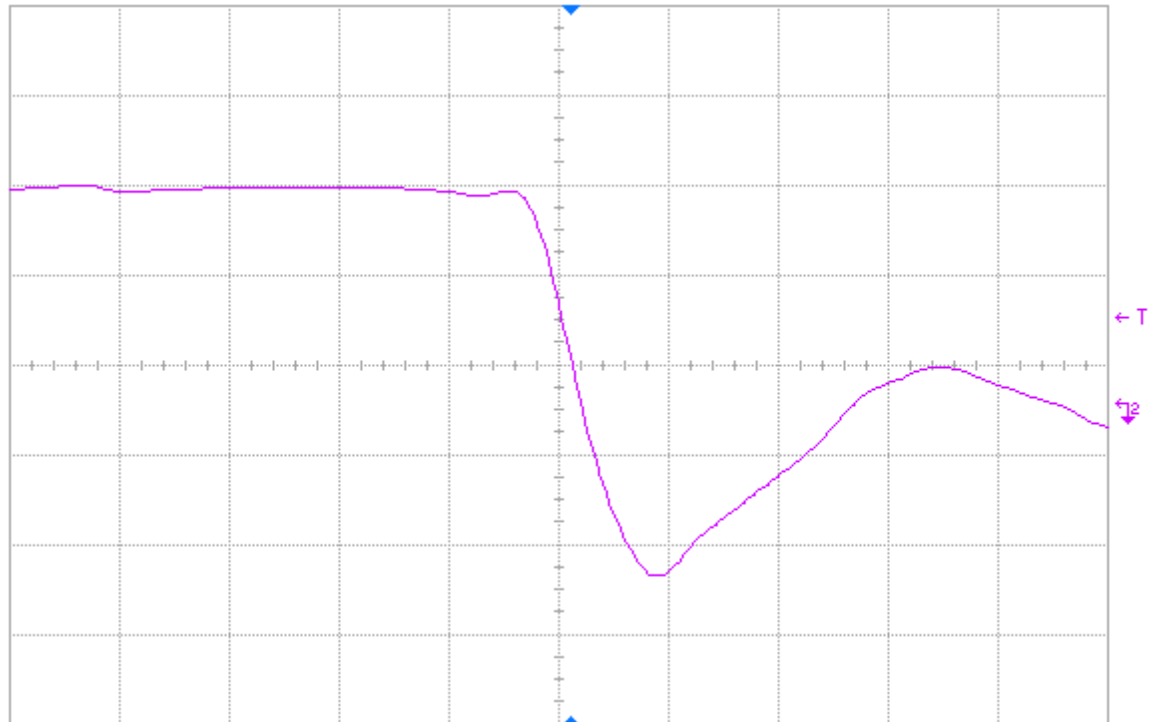
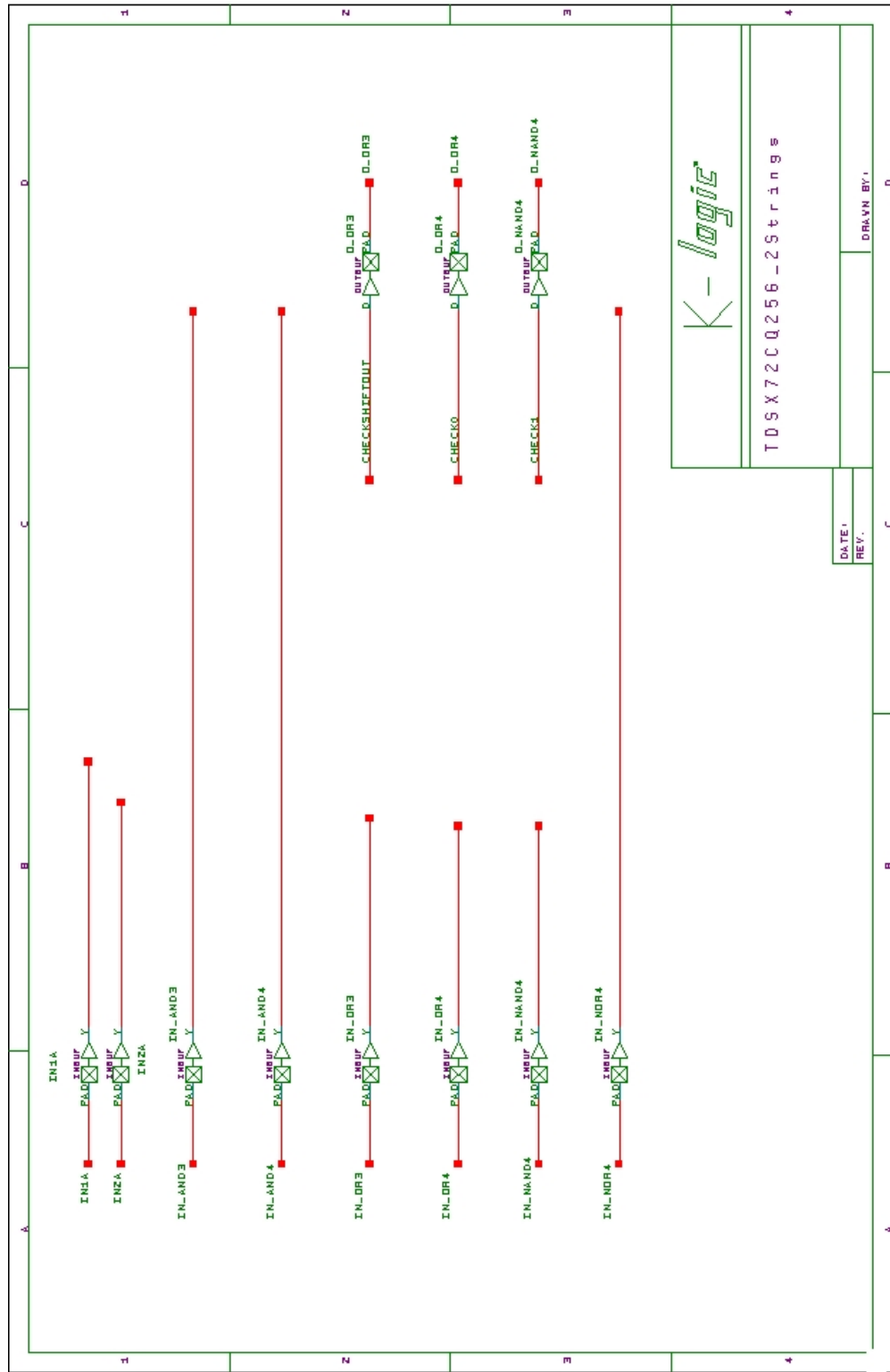
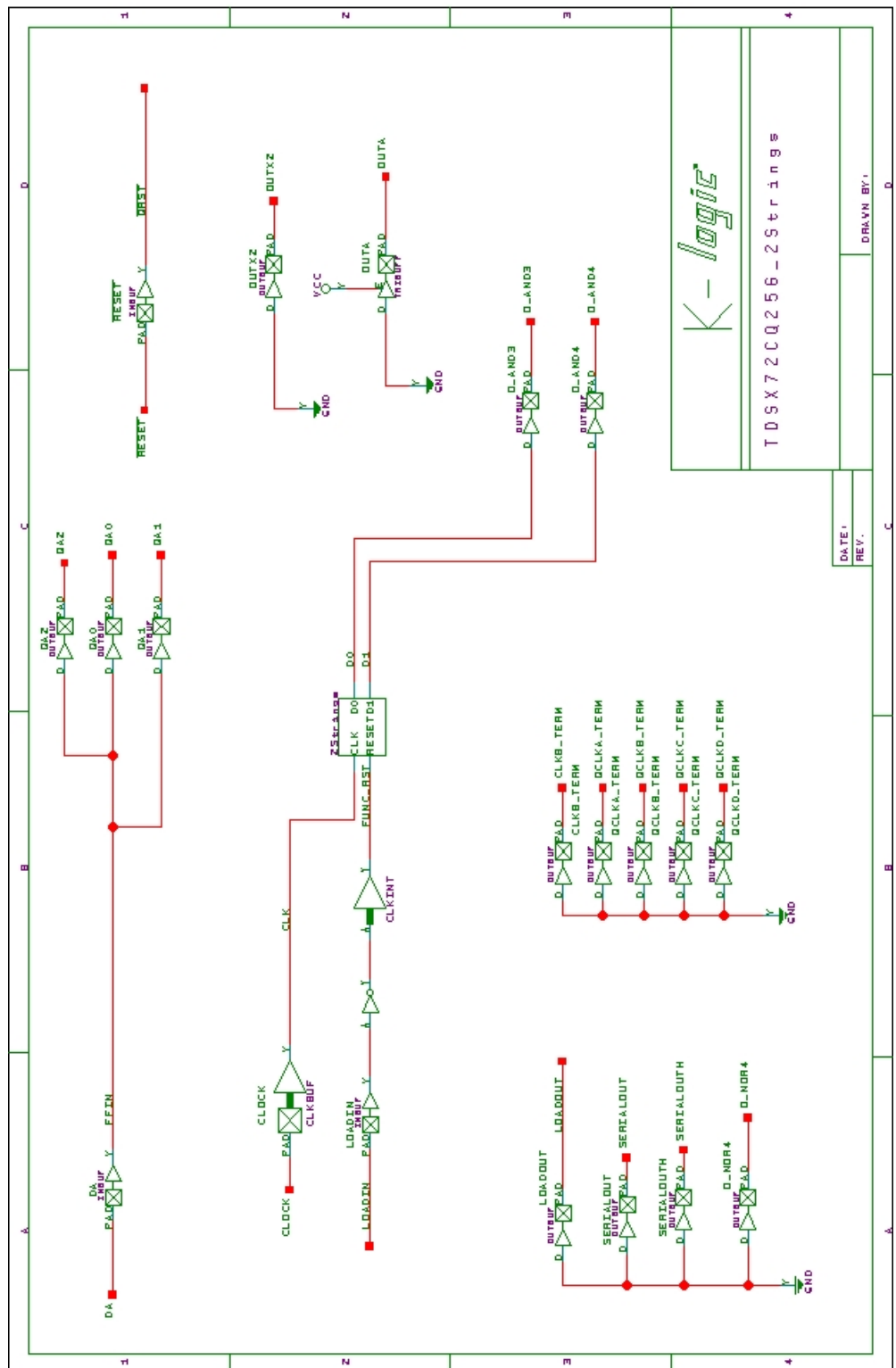
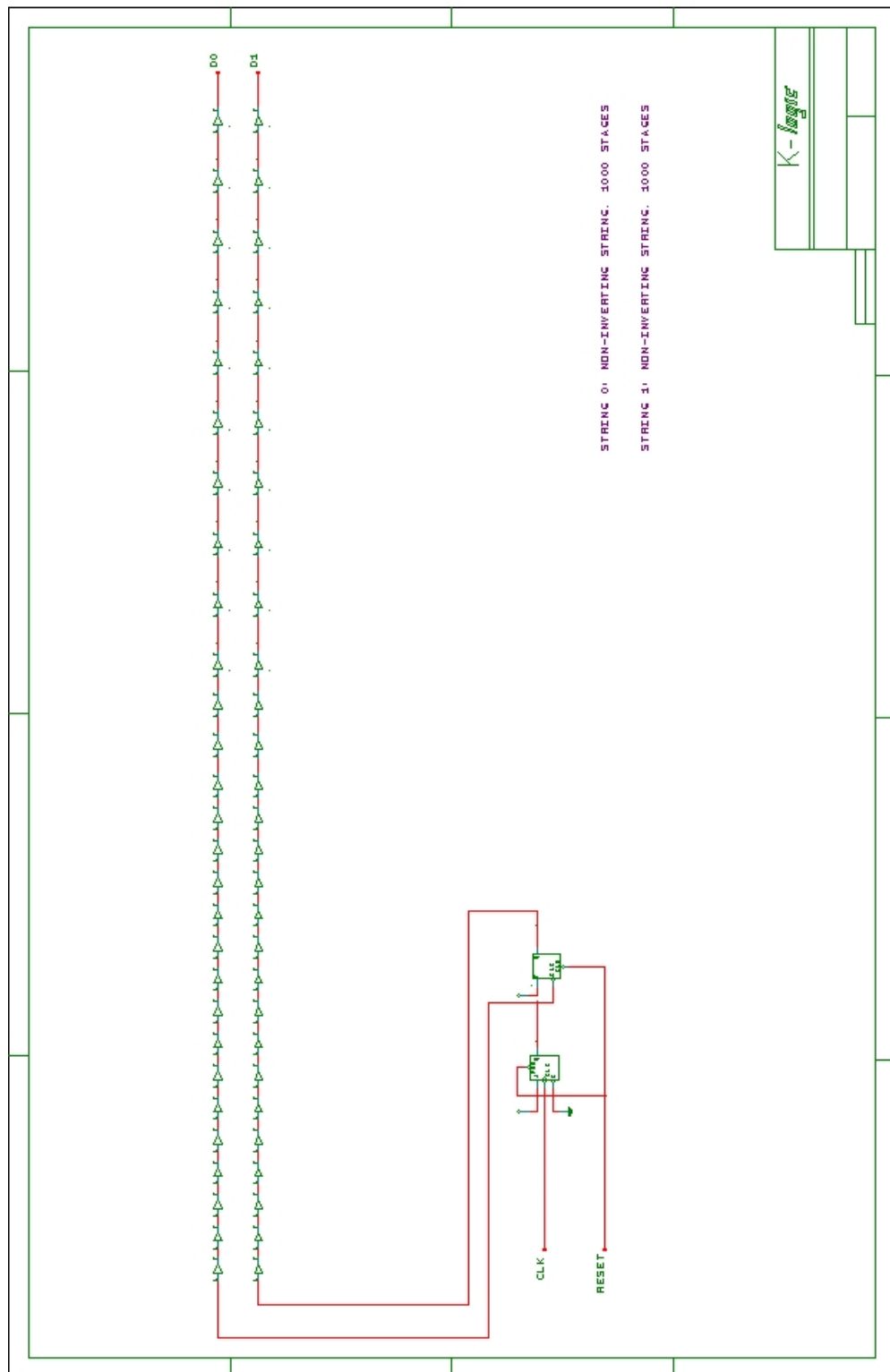


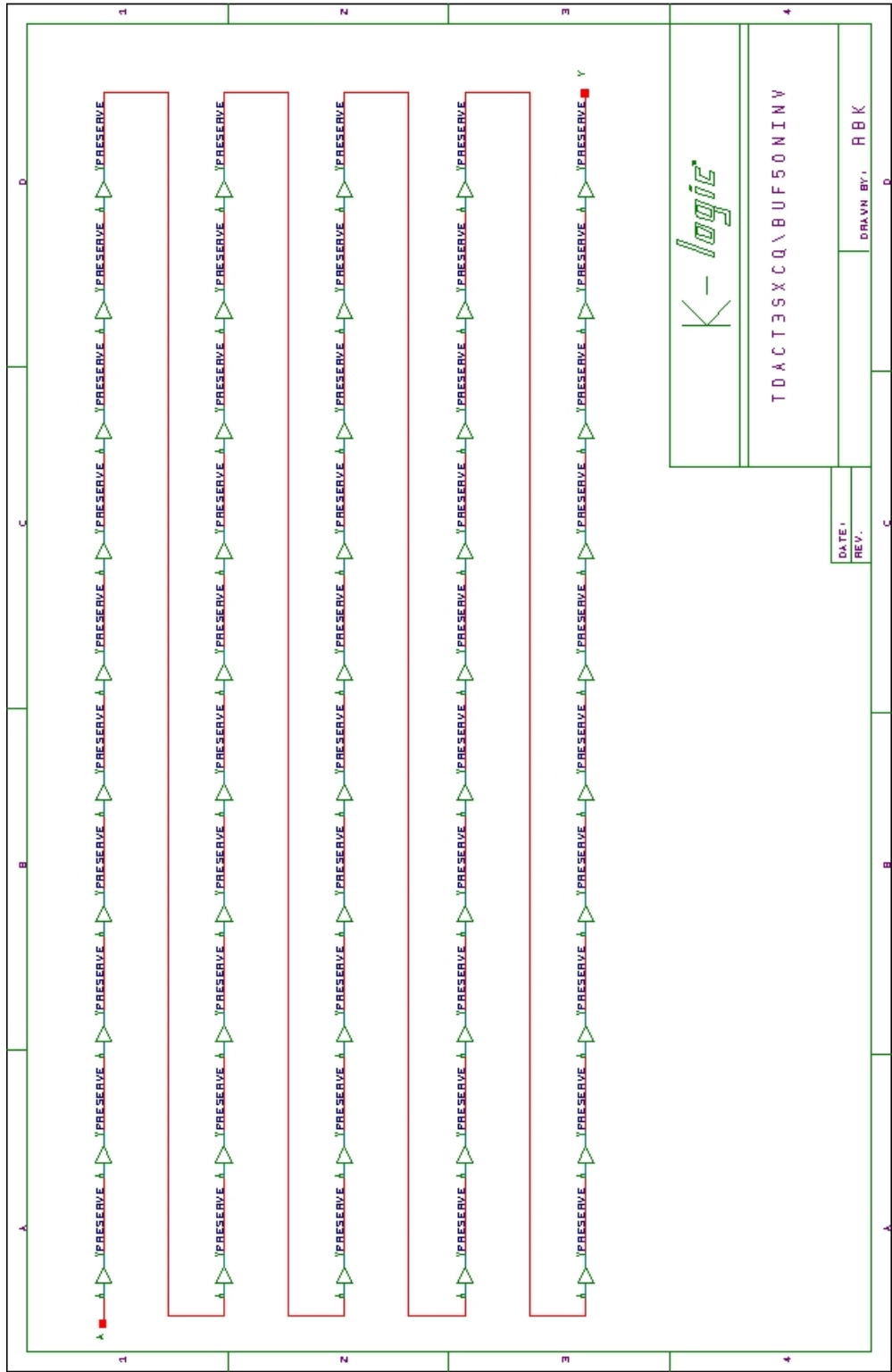
Fig 17(b) Post-annealing falling edge of DUT 13789, abscissa scale is 2 V/div and ordinate scale is 2 ns/div.

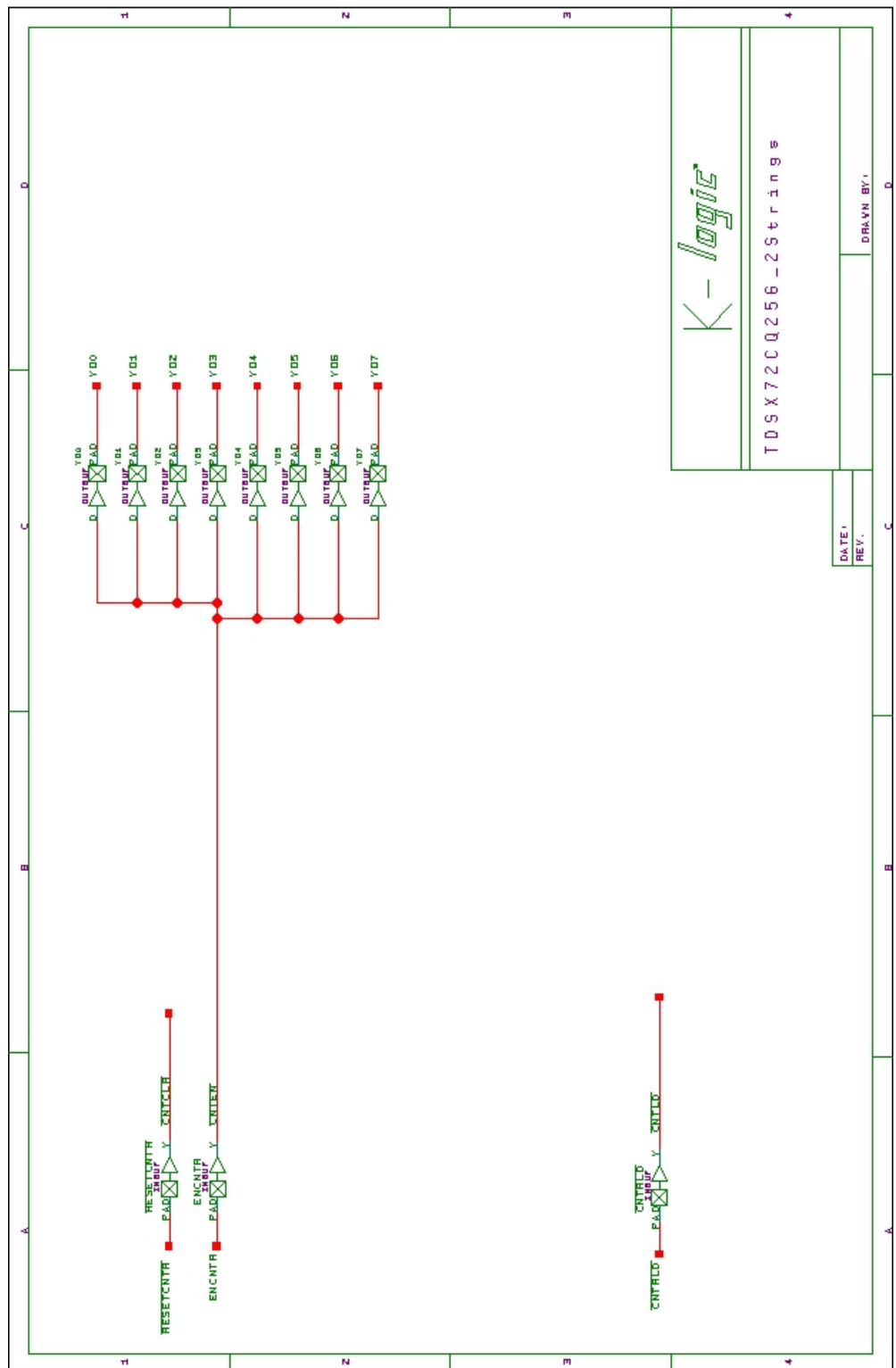
APPENDIX A DUT DESIGN SCHEMATICS

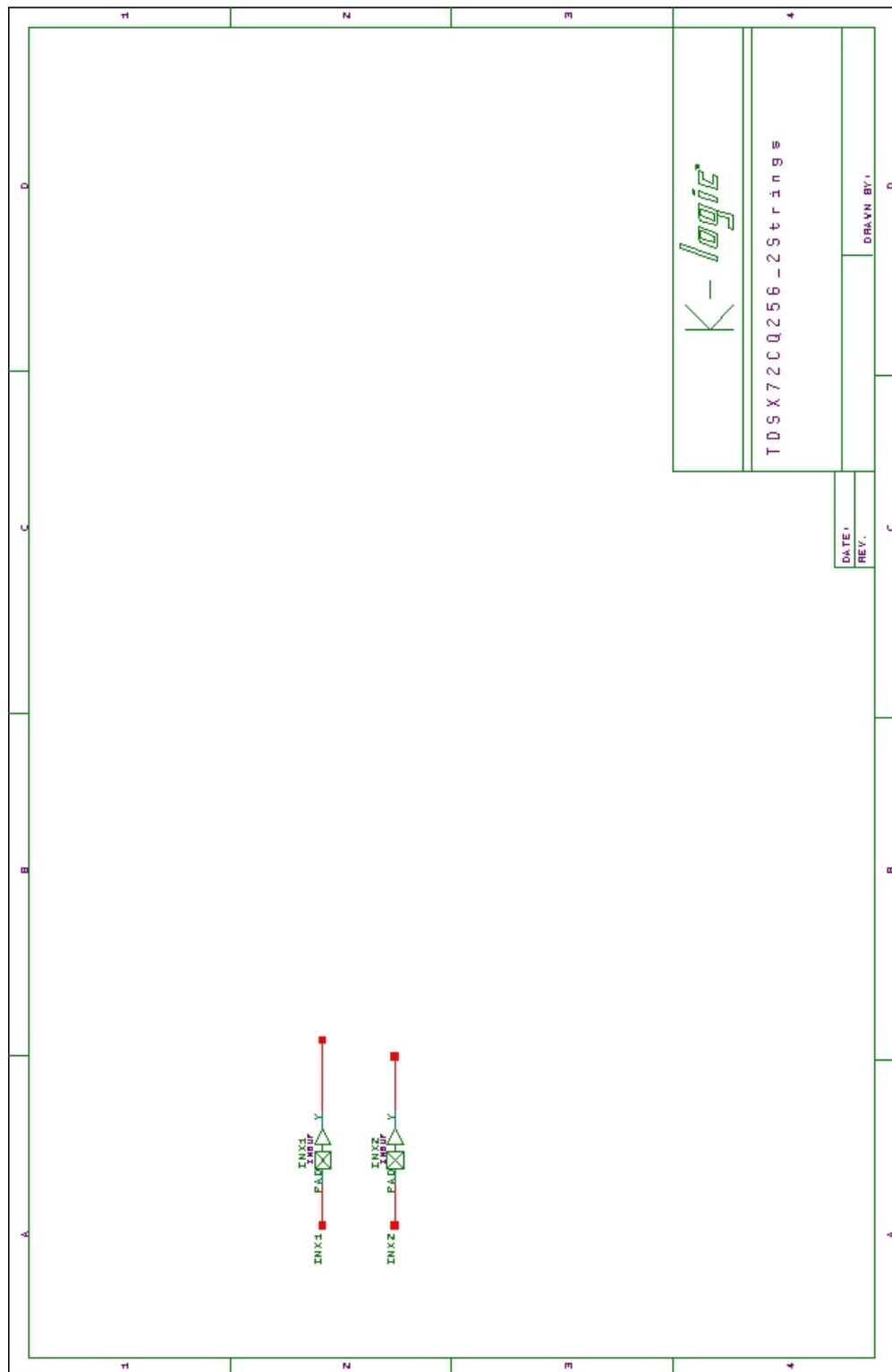


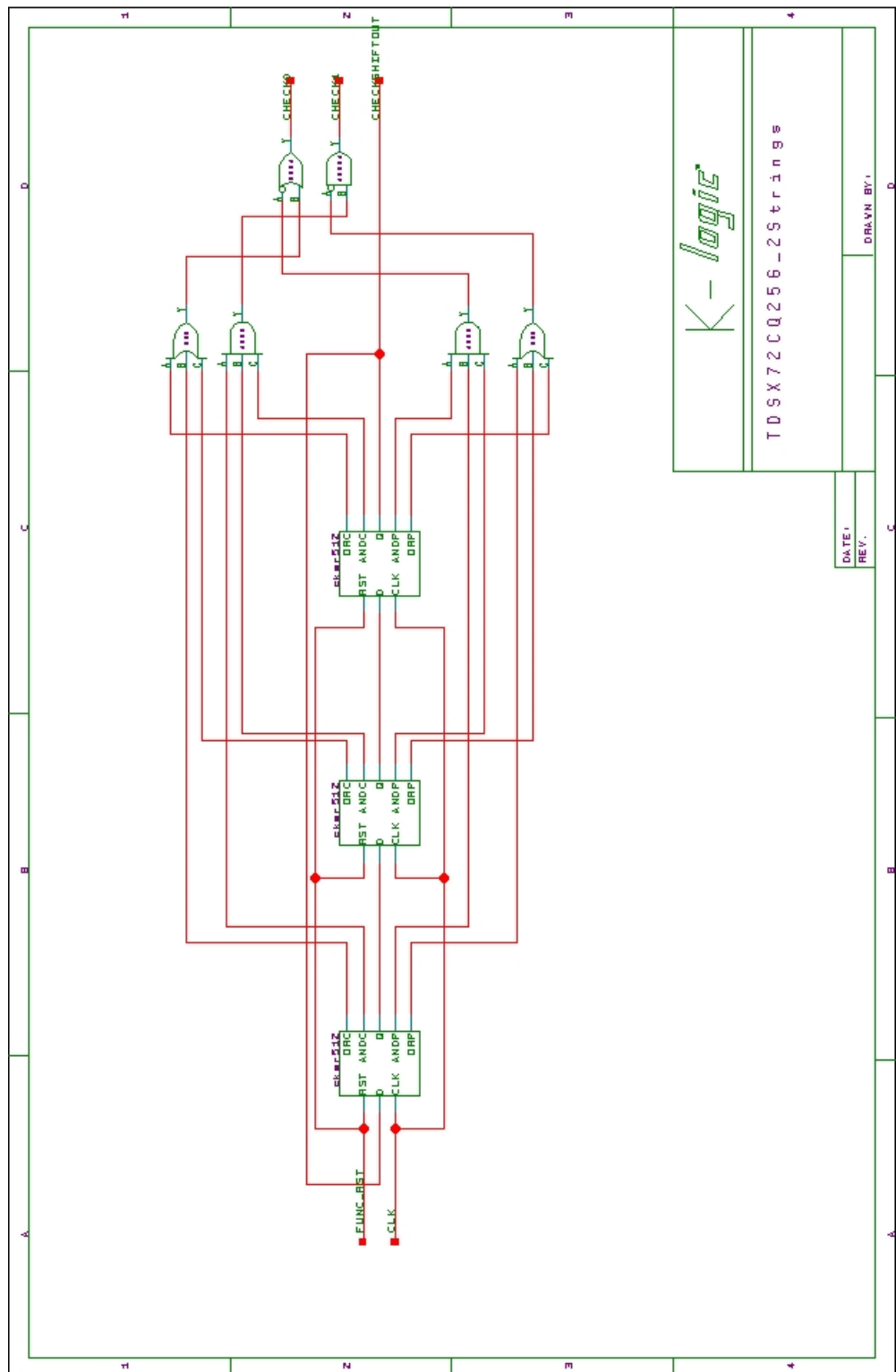


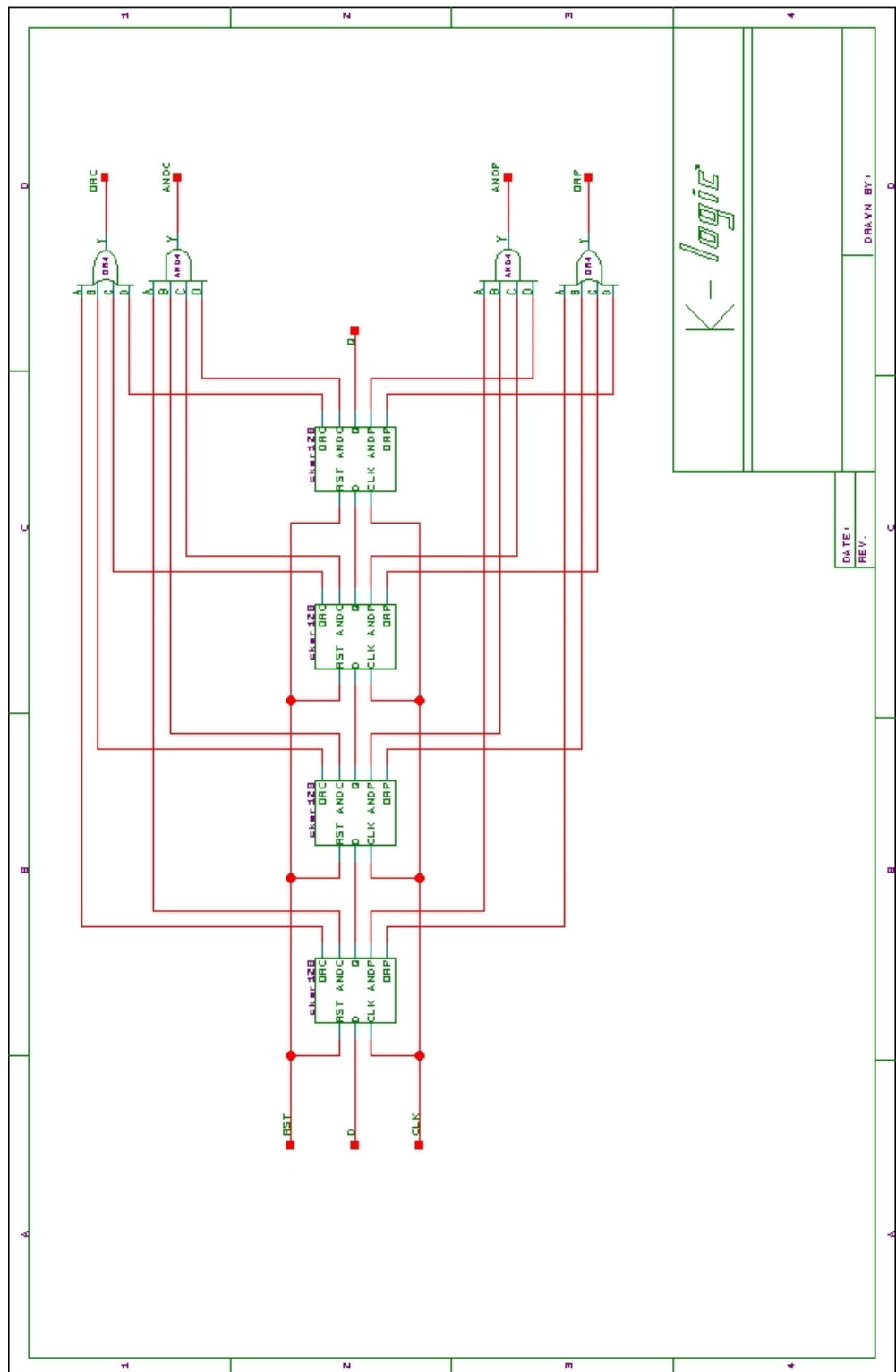


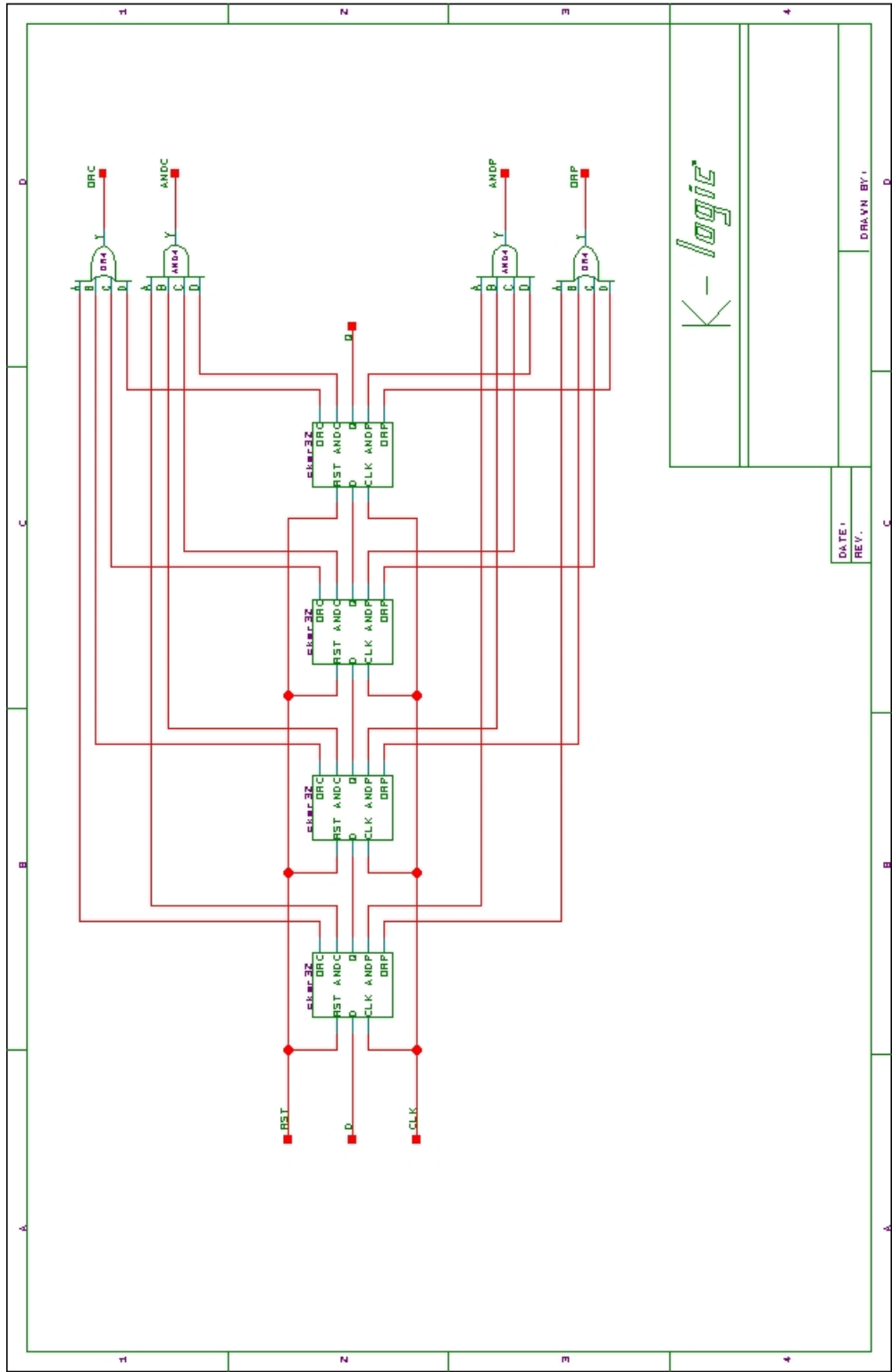


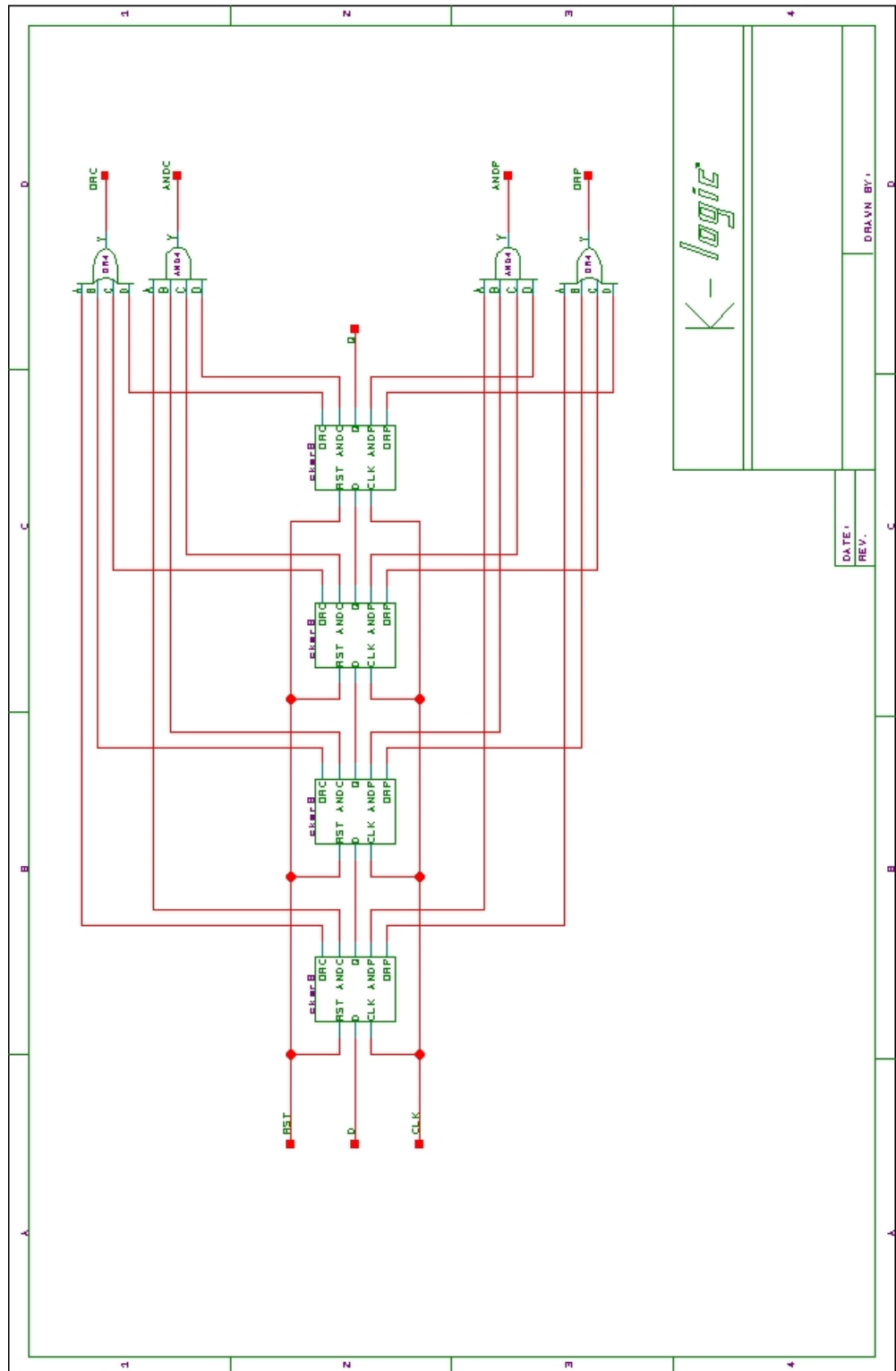


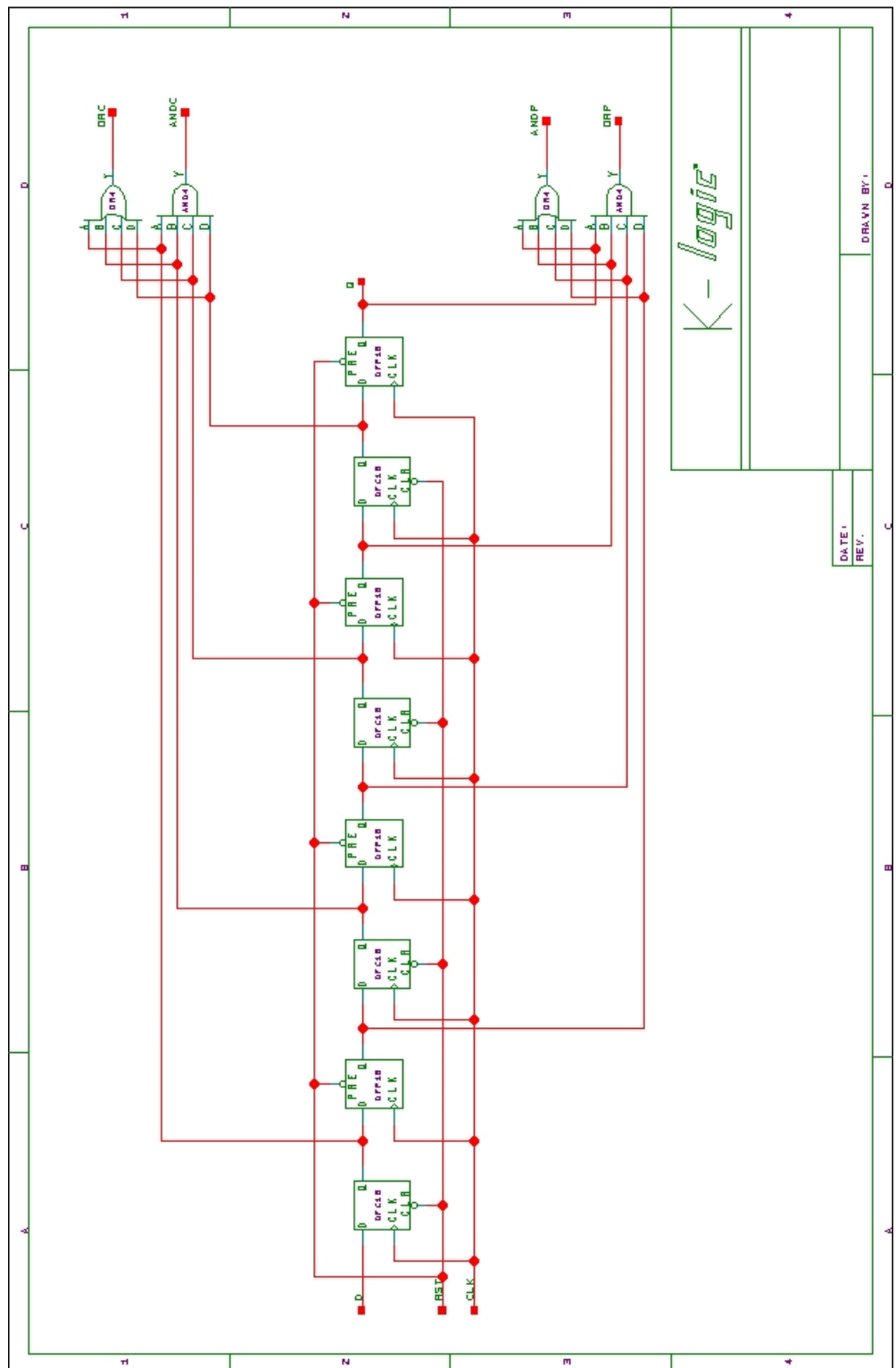


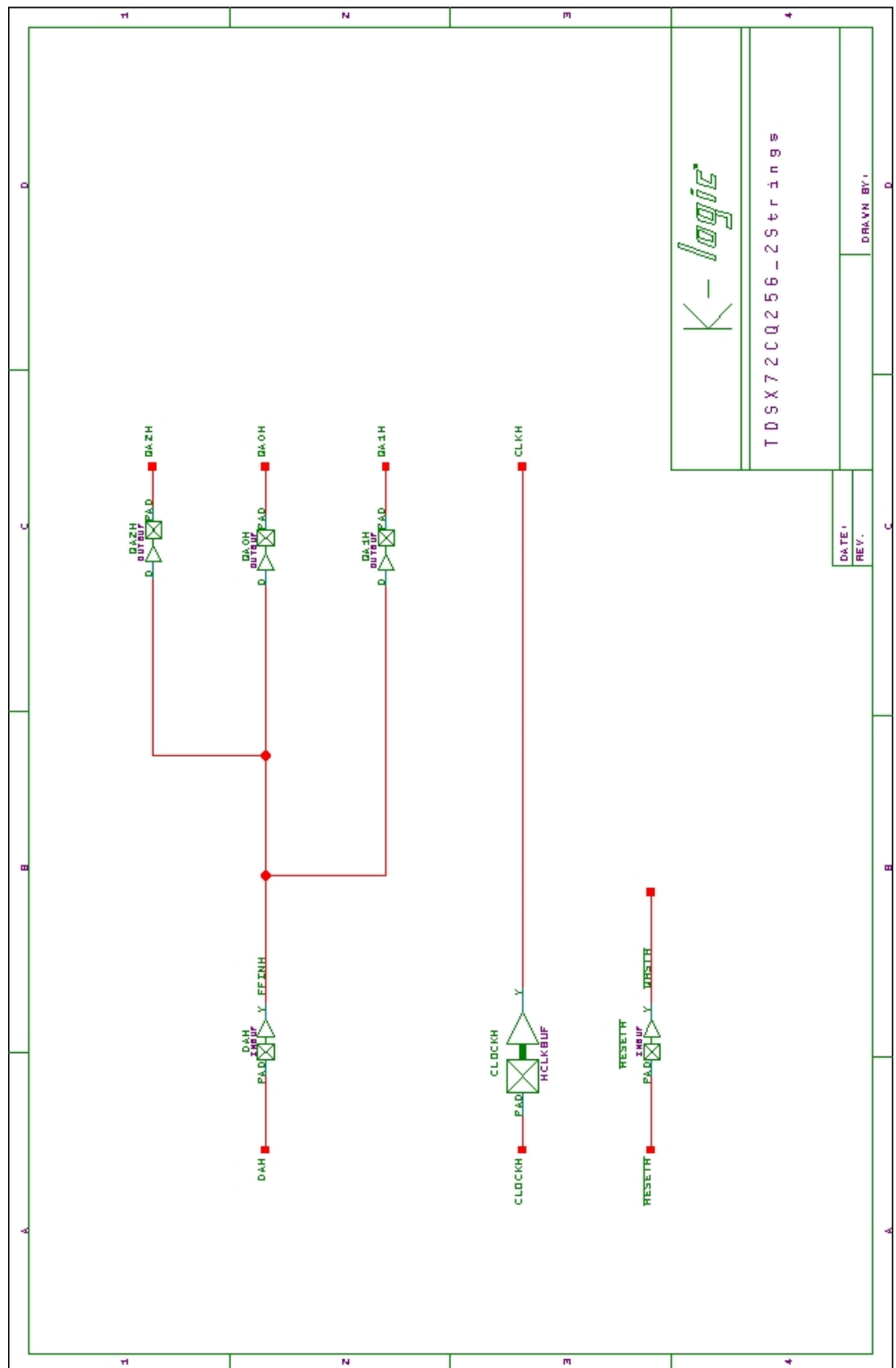


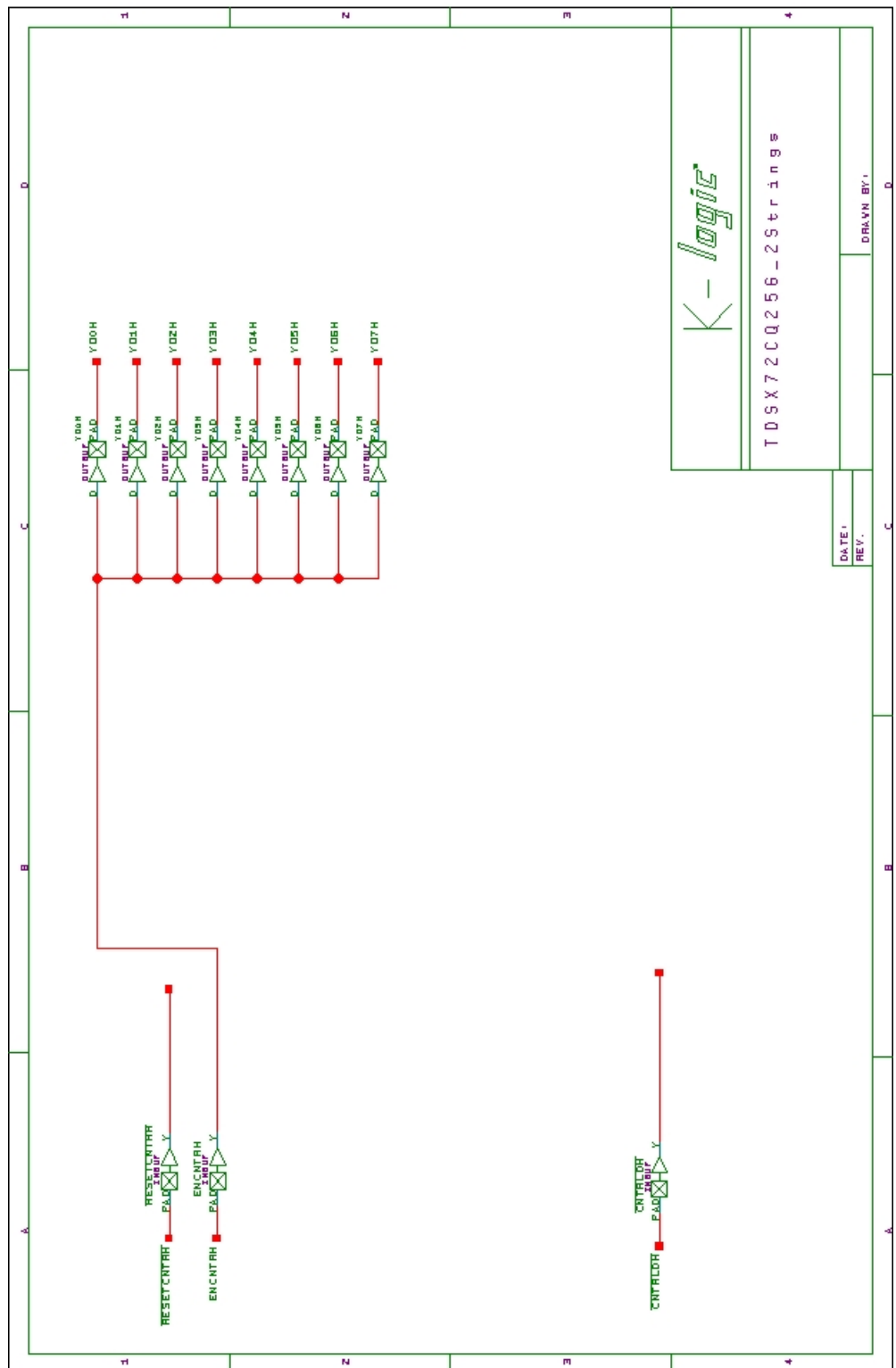


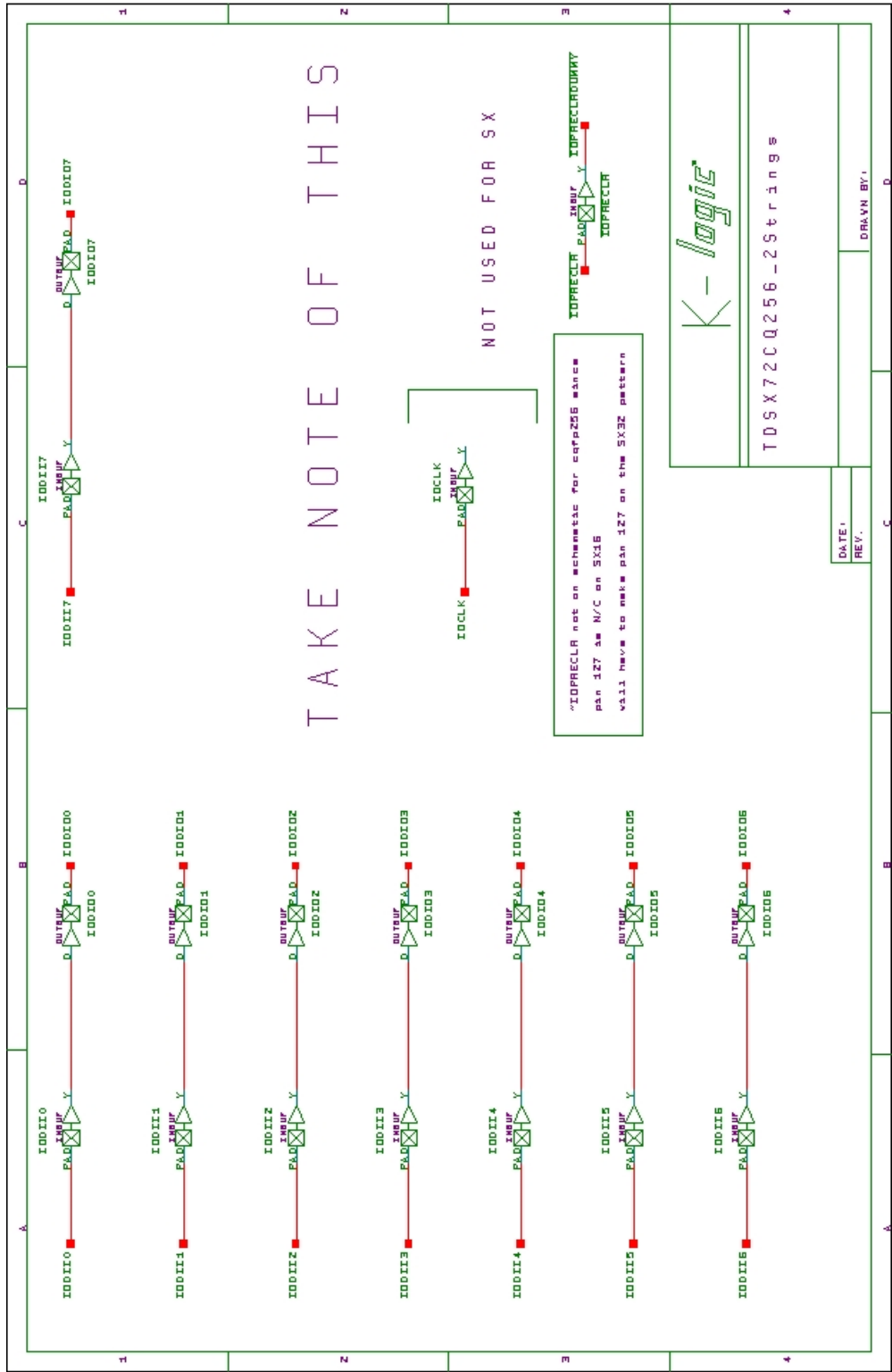












1	2	3	4												
A	B	C	D												
A	B	C	D												
<p style="text-align: center;"><i>K - logiE</i></p> <hr/> <p style="text-align: center;">TDSX72CQ256 - 2S trin gs</p> <hr/> <table border="1" style="width: 100%; border-collapse: collapse;"> <tr> <td style="width: 25%;">DATE:</td> <td style="width: 25%;">REV.:</td> <td style="width: 25%;">DRAWN BY:</td> <td style="width: 25%;">C</td> </tr> <tr> <td> </td> <td> </td> <td> </td> <td>B</td> </tr> <tr> <td> </td> <td> </td> <td> </td> <td>A</td> </tr> </table>				DATE:	REV.:	DRAWN BY:	C				B				A
DATE:	REV.:	DRAWN BY:	C												
			B												
			A												
A	B	C	D												
1	2	3	4												

